LINK QUALITY ANALYSIS OF WIRELESS UNDERGROUND SENSOR NETWORKS

by

Bruno Jorge de Carvalho e Silva

Submitted in partial fulfilment of the requirements for the degree
Master of Engineering (Computer Engineering)

in the

Department of Electrical, Electronic and Computer Engineering
Faculty of Engineering, Built Environment and Information Technology

UNIVERSITY OF PRETORIA

November 2014

SUMMARY

LINK QUALITY ANALYSIS OF WIRELESS UNDERGROUND SENSOR NETWORKS

by

Bruno Jorge de Carvalho e Silva

Supervisor: Dr. G.P. Hancke

Department: Electrical, Electronic and Computer Engineering

University: University of Pretoria

Degree: Master of Engineering (Computer Engineering)

Keywords: Underground sensor networks, underground communication, link quality estimation, protocol development, wireless network, electromagnetic propagation, channel characteristics, wireless testbed

Wireless Sensor Networks have received significant attention due to their capability for distributed sensing at relatively low cost, in applications which range from environmental to industrial monitoring. More recently, wireless underground sensor networks have been proposed for applications such as personnel tracking in underground mines and moisture monitoring for precision agriculture. Wireless underground sensor networks are typically categorised into wireless sensor networks for mines and tunnels (which communicate over-the-air) and Subsoil Wireless underground sensor networks (which communicate wirelessly through soil).

For Subsoil wireless underground sensor networks specifically, it is well known that the soil medium introduces a number of challenges. Firstly, the path loss in soil is very high. Secondly, propagation characteristics are dependent on soil conditions and properties, which can change due to irrigation or rain. Thirdly, communication in Subsoil Wireless underground sensor networks takes place over three different types of channels: underground-to-underground, aboveground-to-underground and underground-to-aboveground. Therefore, communication protocols developed for over-the-air wireless sensor networks are not suitable for wireless underground sensor networks. Although some

studies on wireless underground sensor networks have focussed on channel characterization, many aspects related to link characteristics have not been thoroughly investigated. Understanding the link behaviour in wireless underground sensor networks is a fundamental building block for protocol development for medium access, topology management and routing.

The aim of this research is to gain insight into the link quality in wireless underground sensor networks which can aid in the development of efficient and reliable communication protocols. To this end, the link quality in the three wireless underground sensor network communication channels is characterized empirically for dry and wet soil conditions. This characterization is performed using the received signal strength, link quality indicator and packet reception rate. The results show that links in the underground-to-underground channel are very stable (in terms of received signal strength) and exhibit high symmetry and high packet reception rate, even for received signal strength values near the receiver sensitivity, but the communication ranges are limited due to the very high attenuation. On the other hand, links in the aboveground-to-underground /underground-to-aboveground channels are typically asymmetric and have longer communication ranges. For most links in all three channels, it is observed that the link quality indicator is highly variant and is not correlated with received signal strength and packet reception ratio. Furthermore, an increase in the soil moisture also affects the link asymmetry and the width of the transitional windows in the aboveground-to-underground/underground-to-aboveground channels. The results show that efficient communication protocols for wireless underground sensor networks will have to be highly adaptive/reactive to soil conditions, and link quality estimation has to be robust to the asymmetry present in most links.

OPSOMMING

VERBINDINGKWALITEITANALISE VAN DRAADLOSE ONDERGRONDSE SENSORNETWERKE

deur

Bruno Jorge de Carvalho e Silva

Studieleier: Dr. G.P. Hancke

Departement: Elektriese, Elektroniese en Rekenaaringenieurswese

Universiteit: Universiteit van Pretoria

Graad: Magister in Ingenieurswese (Rekenaaringenieurswese)

Sleutelwoorde: Ondergrondse sensornetwerke, ondergrondse kommunikasie, protokolontwikkeling, draadlose netwerk, elektromagnetiese voortplanting, kanaal-eienskappe, draadlose toetsplatform

Draadlose sensornetwerke geniet heelwat aandag weens hulle vermoë tot verspreide waarneming teen betreklik lae koste in toepassings wat van omgewings- tot industriële monitering strek. In die afgelope tyd word draadlose ondergrondse sensornetwerke voorgestel vir toepassings soos personeelsporing in ondergrondse myne en vogmonitering in presisie-landbou. Draadlose ondergrondse sensornetwerke word tipies ingedeel in draadlose sensornetwerke vir myne en tonnels (wat deur lug kommunikeer) en ondergrondse draadlose ondergrondse sensornetwerke (wat deur grond kommunikeer).

Vir ondergrondse draadlose sensornetwerke in besonder is dit wel bekend dat die grondmedium ernstige uitdagings meebring. Eerstens is die transmissie-verlies in grond baie hoog. Tweedens is voortplantingskenmerke afhanklik van grondtoestande en -eienskappe wat weens besproeiïng of reën kan verander. Derdens vind kommunikasie in ondergrondse draadlose sensornetwerke oor drie verskillende tipes kanale plaas, naamlik ondergronds-tot-ondergronds, bogronds-tot-ondergronds en ondergronds-tot-bogronds. Kommunikasieprotokolle wat vir deur-die-lug-draadlose sensornetwerke ontwikkel is, is dus nie vir draadlose ondergrondse sensornetwerke geskik nie. Alhoewel enkele

ondersoeke na draadlose ondergrondse sensornetwerke op kanaalkarakterisering toegespits was, is baie aspekte in verband met skakelkarakteristieke nie deeglik ondersoek nie. Om die verbindinggedrag in draadlose ondergrondse sensornetwerke te begryp is ’n fundamentele bousteen vir protokolontwikkeling vir mediumtoegang, topologiebestuur en roetering.

Die oogmerk van hierdie navorsing is om insig te verkry in die verbindingkwaliteit in draadlose ondergrondse sensornetwerke wat kan help om doeltreffende en betroubare kommunikasieprotokolle te ontwikkel. Hiervoor word die verbindingkwaliteit in die drie draadlose ondergrondse sensornetwerke-kommunikasiekanale empiries gekarakteriseer vir droë en nat grondtoestande. Hierdie karakterisering word uitgevoer deur gebruik te maak van die ontvangde seinsterkte, verbindingkwaliteitaanduider en pakketontvangstempo. Die resultate toon dat verbindings in die ondergronds-tot-ondergronds-kanaal baie stabiel is (ten opsigte van ontvangde seinsterkte) en toon groot simmetrie en hoë pakketontvangstempo, selfs vir ontvangde seinsterkte-waardes na aan die ontvangergevoeligheid, maar die kommunikasiestrekke is weens die baie hoë verswakking beperk. Andersyds is verbindings in die bogronds-tot-ondergronds en ondergronds-tot-bogronds-kanale tipies asimmetries en het langer kommunikasiesafstande. Daar is opgemerk dat die verbindingkwaliteitaanduider vir meer verbindings in al drie kanale baie wissel en nie met ontvangde seinsterkte of pakketontvangstempo korreleer nie. Verder beïnvloed ’n toename in grondvog ook die verbinding-asimmetrie en die wydte van die oorgangsvensters in die bogronds-tot-ondergronds/ondergronds-tot-bogronds-kanale. Die resultate toon dat doeltreffende kommunikasieprotokolle vir draadlose ondergrondse sensornetwerke hoogs aanpaslik/responsief teenoor grondtoestande moet wees en dat verbindingsberaming robuust moet wees ten opsigte van die asimmetrie wat in die meeste verbindings teenwoordig is.

ACKNOWLEDGEMENTS

I would like to thank:

- Dr. G.P. Hancke and Prof. G.P. Hancke for their guidance and advice, and for giving me the opportunity to complete my MEng under their supervision.
- Dr. Anuj Kumar for his help and advice with all experiments.
- Mr. Burger Cillie and the staff of the Field Trial Unit at the Experimental Farm for facilitating all experiments.
- CeTEIS for granting me a bursary for my postgraduate studies.
- My friends and colleagues (in particular Mohau, Dolly and Rogério) at the ASN research group for all the insightful discussions.
- My family for all the encouragement, advice and support.

LIST OF ABBREVIATIONS

ACK	Acknowledgment
AG2UG	Aboveground-to-underground
ASK	Amplitude Shift Keying
ARQ	Automatic Repeat Request
BER	Bit Error Rate
CER	Chip Error Rate
CRC	Cyclic Redundancy Check
CSMA	Carrier Sense Multiple Access
DLL	Data Link Layer
DSSS	Direct-sequence Spread Spectrum
EHF	Extremely High Frequency
EM	Electromagnetic
ETX	Expected Transmission Count
FEC	Forward Error Correction
FFD	Full Function Device
FSK	Frequency Shift Keying
GSM	Global System for Mobile Communications
LOS	Line-of-sight
LQE	Link Quality Estimation
LQI	Link Quality Indicator
MAC	Medium Access Control
MEMS	Micro Electromechanical Systems
MI	Magnetic Induction

NLOS	Non-line-of-sight
OTA	Over-the-air
PAN	Personal Area Network
PER	Packet Error Rate
PHY	Physical
PSK	Phase Shift Keying
PRR	Packet Reception Ratio
QoS	Quality of Service
RF	Radio Frequency
RFD	Reduced Function Device
RFID	Radio–frequency Identification
RSS	Received Signal Strength
RX	Receive
SINR	Signal-to-interference-plus-noise Ratio
SNR	Signal to Noise Ratio
TDMA	Time Division Multiple Access
TIR	Total Internal Reflection
TX	Transmit
UWB	Ultra-wideband
UG2AG	Underground-to-aboveground
UG2UG	Underground-to-underground
VWC	Volumetric Water Content
WBAN	Wireless Body Area Network
WPAN	Wireless Personal Area Network
WSN	Wireless Sensor Network
WUSN	Wireless Underground Sensor Network

LIST OF TABLES

Table 2.1: Motes' hardware specifications (data sourced from devices' datasheets) 8
Table 2.2: ZigBee, WirelessHART and ISA100.11a comparison. 17
Table 2.3: Comparison of DASH7 and ZigBee (based on information from [43]) 19
Table 2.4: Examples of WSN applications. 20
Table 5.1: Simulation parameters for Castalia. 47
Table 5.2: Transceiver configuration. 50
Table 5.3: Soil sample analysis results. 51
Table 5.4: Specifications of antennas used in experiments. 53
Table 6.1: Typical RSS and LQI variance for 3 different environments. 65
Table 6.2: Asymmetry for the UG2UG channel. 67
Table 6.3: Comparison of RSS for wet and dry scenarios. 68
Table 6.4: Asymmetry for UG2AG and AG2UG links. 72

LIST OF FIGURES

Figure 1.1: Link quality in the WSN protocol stack..... 3
Figure 2.1: Sensor node architecture. 7
Figure 2.2: Multi-hop routing in WSNs. 9
Figure 2.3: Flooding in WSNs..... 13
Figure 2.4: Topologies in ZigBee networks. 15
Figure 3.1: A WUSN for irrigation management. 23
Figure 3.2: Path loss for OTA WSN. 24
Figure 3.3: Path loss for WUSN with 5% VWC. 25
Figure 3.4: UG2UG Channel. 30
Figure 3.5: UG2AG Channel. 32
Figure 3.6: AG2UG Channel. 32
Figure 4.1: Packet Reception Ratio for frame lengths of 20, 50 and 127 bytes. 36
Figure 4.2: Hardware and software based estimators. 42
Figure 5.1: Node placement for 4 destination nodes. 46
Figure 5.2: Interface between Castalia and MATLAB..... 47
Figure 5.3: Test-bed configuration. 48
Figure 5.4: Experimental site at the Experimental Farm. 49
Figure 5.5: Hole topology for experiments. 49
Figure 5.6: Sink node in a) and an unburied node in b). 55
Figure 5.7: Software flow diagrams for sink and source nodes. 56
Figure 5.8: Effect of antenna height on RSS. 57
Figure 5.9: Testing scenario for UG2AG and UG2AG experiments. 57
Figure 6.1: PRR vs inter-node distance for UG2UG link..... 59
Figure 6.2: Indoor testing scenario. 60
Figure 6.3: Indoor RSS temporal characteristics for links 1 and 2..... 61
Figure 6.4: Indoor LQI temporal characteristics for links 1 and 2. 61
Figure 6.5: Outdoor RSS temporal characteristics. 62
Figure 6.6: Outdoor LQI temporal characteristics..... 63
Figure 6.7: UG2UG RSS temporal characteristics. 64
Figure 6.8: UG2UG RSS spatial characteristics. 64
Figure 6.9: LQI temporal characteristics. 65

Figure 6.10: LQI spatial characteristics. 66
Figure 6.11: Forward and reverse PRRs for UG2UG links. 67
Figure 6.12: AG2UG/UG2AG RSS temporal characteristics. 69
Figure 6.13: AG2UG/UG2AG RSS spatial characteristics. 70
Figure 6.14: AG2UG/UG2AG LQI temporal characteristics for 1 meter. 70
Figure 6.15: AG2UG/UG2AG LQI spatial characteristics. 71
Figure 6.16: PRR for UG2AG and AG2UG links. 72

TABLE OF CONTENTS

CHAPTER 1 INTRODUCTION 1

1.1 OVERVIEW 1

1.2 MOTIVATION 2

1.3 OBJECTIVES 4

1.4 RESEARCH QUESTIONS 4

1.5 RESEARCH CONTRIBUTION 5

1.6 THESIS OUTLINE 5

CHAPTER 2 WIRELESS SENSOR NETWORKS 7

2.1 INTRODUCTION 7

2.2 COMMUNICATION PROTOCOLS 9

2.2.1 Physical Layer 9

2.2.2 Data Link Layer and Medium Access 10

2.2.3 Network Layer 12

2.2.4 Transport and Application Layers 14

2.3 WIRELESS SENSOR NETWORK STANDARDS 14

2.3.1 802.15.4 and ZigBee 14

2.3.2 WirelessHART and ISA100.11a 16

2.3.3 DASH7 18

2.3.4 Other Wireless Communication Standards 19

2.4 APPLICATIONS 20

CHAPTER 3 WIRELESS UNDERGROUND SENSOR NETWORKS 22

3.1 INTRODUCTION 22

3.2 WUSN CLASSIFICATION 22

3.3 WIRELESS PROPAGATION IN SOIL 23

3.3.1 Soil Properties 25

3.3.2 Modelling Wireless Propagation in Soil 26

3.3.3 Impact of Soil on Propagation Characteristics 27

3.4 PROPAGATION MODELS 28

3.4.1 UG2UG Channel 29

3.4.2 AG2UG and UG2AG Channels 30
3.5 ALTERNATIVE COMMUNICATION APPROACHES 33

CHAPTER 4 LINK QUALITY ESTIMATION 35
4.1 INTRODUCTION 35
4.2 AN OVERVIEW OF LINK QUALITY ESTIMATION 35
4.2.1 Link Quality Modelling 35
4.2.2 The Process of Link Quality Estimation 36
4.3 HARDWARE BASED LINK QUALITY ESTIMATORS 37
4.3.1 Received Signal Strength and Signal to Noise Ratio 37
4.3.2 Link Quality Indicator 38
4.3.3 The Triangle Metric 38
4.4 SOFTWARE BASED LINK QUALITY ESTIMATORS 39
4.4.1 PRR 39
4.4.2 ETX 40
4.4.3 RNP 40
4.4.4 4-bit 41
4.4.5 F-LQE 41
4.4.6 ETF 42
4.4.7 Interference Aware Metrics 43

CHAPTER 5 DESCRIPTION OF EXPERIMENTS 44
5.1 INTRODUCTION 44
5.2 SIMULATION SETUP 44
5.2.1 Overview of Simulators 44
5.2.2 Simulation Details 45
5.3 EXPERIMENTAL SETUP 48
5.3.1 Test-bed Configuration 48
5.3.2 Transceiver Configuration 49
5.3.3 Soil Characterization 50
5.3.4 Antenna Selection 51
5.3.5 Experimental Protocol 54
5.3.6 Software Description 55
5.3.7 The AG2UG and UG2AG Test Protocol 56

CHAPTER 6 RESULTS AND DISCUSSION 59
6.1 INTRODUCTION 59
6.2 SIMULATION RESULTS 59
6.3 ABOVEGROUND EXPERIMENTAL RESULTS 60
6.3.1 Indoor Experiments 60
6.3.2 Outdoor Experiments 62
6.4 UNDERGROUND-TO-UNDERGROUND RESULTS 63
6.4.1 RSS Temporal and Spatial Characteristics 63
6.4.2 LQI Temporal and Spatial Characteristics 65
6.4.3 PRR and Link Asymmetry 66
6.4.4 RSS, LQI and PRR in Wet Scenario 68
6.5 UNDERGROUND-TO-ABOVEGROUND AND ABOVEGROUND-TO-UNDERGROUND RESULTS 68
6.5.1 RSS Temporal and Spatial Characteristics 69
6.5.2 LQI Temporal and Spatial Characteristics 70
6.5.3 PRR and Link Asymmetry 71
6.5.4 RSS, LQI and PRR in Wet Scenario 73
6.6 SUMMARY OF RESULTS 73

CHAPTER 7 CONCLUSION AND FUTURE RESEARCH 74
7.1 CONCLUSION 74
7.2 FUTURE RESEARCH 75

APPENDIX A EQUATIONS FOR DETERMINATION OF SOIL PARAMETERS 85

CHAPTER 1 INTRODUCTION

1.1 OVERVIEW

With recent advances in technology enabling ubiquitous computing and internet-of-things (IoT), research on wireless sensor networks (WSNs) has been instrumental [1] to these developments and the field has been recognised as one of the most active research fields to emerge in recent years [2]. Advances in micro-electrical mechanical systems (MEMS) have inspired research efforts such as Smart Dust [3], whose concept is considered the holy grail of WSNs. WSNs play a fundamental role in IoT, as they enable ubiquitous sensing, a vital component of present and future applications in smart cities [4, 5] and various other environments. It is predicted that the market has the potential to exceed 1 billion in device shipments by 2017 [6].

Although deployments of WSNs are typically done indoors (residential buildings and office environments) or outdoors, where typical applications include environmental monitoring (i.e. monitoring of air pollution and noise levels), there has recently been significant interest from the research community to expand the benefits of WSNs to other environments such as underwater and underground, where the communication medium is no longer air, but is water and soil, respectively. This transition introduces a number of challenges [7, 8] as most research within the WSN field has focussed on wireless communication over-the-air (OTA), and communication protocols have been developed for traditional OTA wireless communication. These new monitoring environments often require novel approaches, and an example of such is the use of acoustic communication for underwater wireless sensor networks, where it has been established that radio frequency (RF) based communication is not feasible.

Wireless underground sensor networks (WUSNs) consist of nodes deployed in the ground (i.e. buried in soil) which communicate between themselves and nodes located aboveground. WUSNs have been envisioned for various applications, such as precision agriculture, monitoring of golf courses' irrigation, and underground pipeline monitoring. In smart irrigation, monitoring the correct parameters (eg. soil moisture) and automating the

irrigation process can result in significant water usage reductions. However, most of the current approaches for smart irrigation systems usually comprise a buried moisture sensor that is attached to a node located aboveground via a cable. WUSNs aim to eliminate the need for cables by using a buried wireless sensor, enabling wireless communication through soil to the sink located aboveground.

Attaining reliable communication in such media is difficult due to the high path loss and dynamic channel conditions which have been reported in numerous studies [9, 10, 11, 12, 13, 14]. Deployment of WUSNs requires further understanding of the soil medium for electromagnetic (EM) based communication. Although some recent work has focussed on channel modelling for EM based WUSNs, further insight into the link quality of the three communication channels in WUSNs is vital towards development of efficient communication protocols.

1.2 MOTIVATION

The development of efficient communication protocols for WUSNs requires further insight into the link characteristics of WUSNs. Although a number of theoretical studies have proposed channel and propagation models, only a few experimental studies have been performed [13, 14]. In particular, to the best of our knowledge, there hasn't been any significant research with regards to link quality characterization and estimation in WUSNs, even though similar research has been conducted for aboveground WSNs. Therefore, we aim to experimentally characterize the link quality of WUSN channels, and gain insight into the differences between the link quality in WUSNs' channels and traditional OTA channels in WSNs. Link quality estimation (LQE) has been established as a fundamental building block for WSNs, in both medium access control (MAC) and routing protocols [15]. Figure 1.1 illustrates the usage of link quality at different layers of the WSN protocol stack.

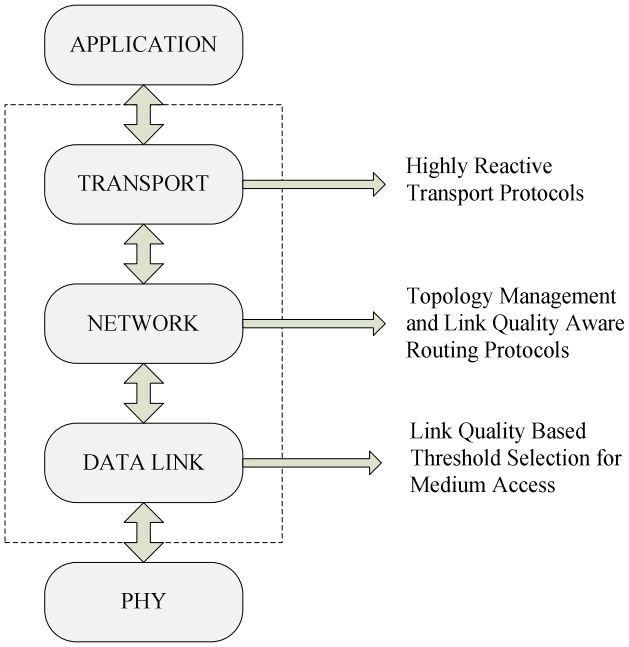

Figure 1.1: Link quality in the WSN protocol stack.

The availability of link quality information in a network improves [15]:

- *Medium Access*: thresholds required for medium access can be computed from link quality metrics which accurately reflect the link state.
- *Topology Management*: nodes in a WSN can rank their neighbours by considering link quality, and only select high quality neighbours for topology establishment, resulting in efficient and stable topologies.
- *Multi-Hop Routing:* a node can measure the link quality to each of its neighbours and select a next hop neighbour with a high link quality (instead of using a naïve metric such as hop-count), therefore selecting next hops with high probability of successful packet delivery.
- *Transport Protocols:* link quality can be used in transport protocols by exploiting spatial and temporal properties in WSNs, enabling highly reactive adaptive transport protocols.

Although some aspects regarding communication (from a data link layer and routing perspective) in WUSNs have been investigated [12, 16, 17, 18], none of these investigations focussed specifically on characterising the link quality in WUSNs. The high

path loss in WUSNs coupled with the relatively weak signals transmitted by low power radios on sensor nodes, and the effects of non-isotropic antennas' radiation patterns [19], contributes to the adverse effects experienced in underground communication. To this end, link behaviour in WUSNs has to be characterized to enable the development of more robust and reliable communication protocols.

In this thesis, WUSN links are characterized in terms of received signal strength (RSS), link quality indicator (LQI) and packet reception ratio (PRR). The most basic metric for link quality assessment is RSS since it is easily available on all transceivers. LQI, on the other hand, is not available in all transceivers, is highly variant, and it requires a large estimation window to perform estimation, which in turn results in an estimator that is slow to adapt. Nevertheless, this high variance property has been exploited for link quality assessment [20]. PRR is considered the most accurate link quality estimator as it can reflect the real link state and is not affected by hardware calibration errors. In particular, RSS can result in a high value in the presence of interference, leading to a high quality assessment for a link which might have a low PRR; LQI has been shown to be highly variant hence requiring large estimation windows; and PRR has less granularity over RSS and LQI. Therefore, link quality characterization using these three metrics is preferable to using only a single metric.

1.3 OBJECTIVES

The objective of this work is to characterize the link quality of WUSN communication channels experimentally. Since the traditional wireless communication channel (i.e. OTA) has enjoyed extensive research, both from a theoretical and experimental perspective, link quality estimation in traditional WSNs is relatively well understood. However, this is not directly applicable to WUSNs, mainly due to the fact that WUSN channels differ from OTA channels. Therefore, this work aims to fill this gap.

1.4 RESEARCH QUESTIONS

The research questions are:

- What are the temporal and spatial characteristics of the three WUSN communication channels with regards to link quality?
- Are current link quality estimators used in WSNs suitable for WUSNs?
- What are the impacts of link quality characteristics of the three channels on protocol development for WUSNs?

1.5 RESEARCH CONTRIBUTION

The contributions of this work are: a framework for WUSN test-bed design and implementation is presented, as well as novel results on the link quality temporal and spatial characteristics for three WUSN channels, in both dry and wet soil conditions. The results of this work will contribute towards a better understanding of link quality estimation in WSNs and will serve as a basis for future link quality estimators, as well as protocol development for WUSNs. The following papers have been published during the course of this research:

1. G.P. Hancke, B.J. de Carvalho e Silva and G.P. Hancke Jr., "The Role of Advanced Sensing in Smart Cities", Sensors, 13, pp. 393 – 425, 2013.
2. B.J. Silva and G.P. Hancke, "On Link Quality Aware Routing for Industrial Wireless Sensor Networks", IEEE ICIT, 25 – 27 Feb. 2013.
3. B.J. Silva and G.P. Hancke, "Link Quality Aware Routing in Wireless Underground Sensor Networks", SATNAC, Sep. 2012.

1.6 THESIS OUTLINE

This thesis is arranged as follows. The first chapter introduces, motivates and describes this research.

Chapter 2 introduces the concept of wireless sensor networks, and presents an overview of standards, communication protocols and applications.

Chapter 3 presents wireless underground sensor networks' channel characteristics, and discusses the main differences between WSNs and EM-based WUSNs.

Chapter 4 provides an overview and state-of-the-art of link quality estimation.

In Chapter 5, the experimental setup, the test-bed configuration and the experimental protocol are described.

The results are analysed and discussed in Chapter 6.

Finally, the thesis is concluded in Chapter 7, where guidelines for future work are proposed.

CHAPTER 2 WIRELESS SENSOR NETWORKS

2.1 INTRODUCTION

Recently, the field of WSNs has received significant attention from the research community for a variety of applications [1, 21, 22]. At a basic level, WSNs consist of inter-connected nodes, also known as motes, equipped with a power supply, low power processing unit (microcontroller), memory, RF transceiver, an antenna, and a set of on-board sensors as illustrated in Figure 2.1.

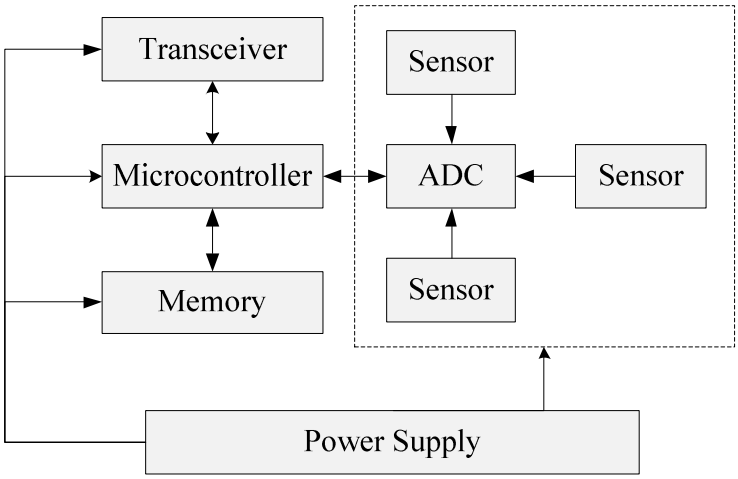

Figure 2.1: Sensor node architecture**.**

The main goal of these networks is to collectively sense some physical phenomena, such as temperature, humidity or vibration, and report all the collected data to a sink, where the data can be subsequently processed and analysed. Table 2.1 contains some hardware specifications of popular motes used in research.

A typical multi-hop WSN scenario is illustrated in Figure 2.2. In this kind of topology, nodes send their information to the sink via multiple hops. As the components used in WSNs are usually low power and communication ranges are limited, these networks are based on multi-hop routing. This allows nodes to save energy by communicating over relatively short hops, as a direct hop to the sink would increase energy expenditure.

Ultimately, for WSNs, it is desirable to keep the components' cost and energy consumption as low as possible because (i) for large-scale WSNs, the deployment cost can become prohibitive, and (ii) some nodes can be deployed in areas where it is unfeasible to replace batteries.

Table 2.1: Motes' hardware specifications (data sourced from devices' datasheets)

Hardware	**I-Mote**	**Mica2**	**Iris**	**Sunspot**	**Waspmote**	**I-Mote2**
Microcontroller	32 bit ARM 12 MHZ	ATmega 128 10 MHz	ATmega 128 10 MHz	ARM920T 180 MHz	ATmega 128 10 MHz	ARM11 400 MHz
Transceiver	Bluetooth	Chipcon CC1000 868/916 MHz	AT86RF230 2.4 GHz	Chipcon CC2420 2.4 GHz	DigiMesh 868/914/2400 MHz	Chipcon CC2420 2.4 GHz
Memory (SRAM/FLASH)	64 K/512 K	4 K/ 128 K	8 K/128 K	512 K/ 4 MB	8 K/128 K	256 K/32 MB

The ideal WSN mote is a low cost, low power sensor node that has no battery, sources power from ambient energy, and has few active components. In the pursuit of this goal, there is significant research on vibration energy harvesting, electromagnetic energy harvesting and other harvesting techniques [23].

WSN nodes can also act as actuators, enabling wireless sensor actor networks, which are commonly used in industrial applications, and consist of some nodes which base their actions on the sensed data.

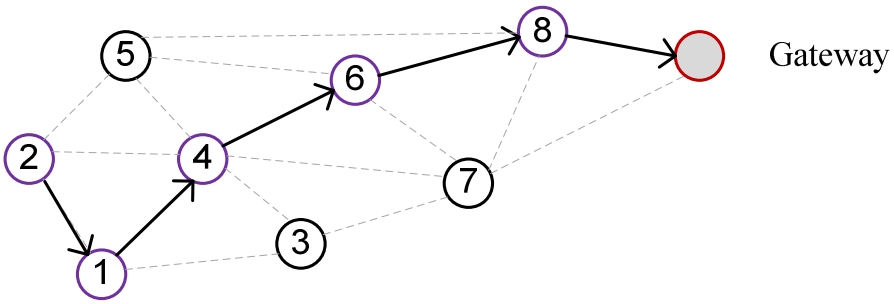

Figure 2.2: Multi-hop routing in WSNs.

2.2 COMMUNICATION PROTOCOLS

Since WSN nodes are typically low power and low cost, novel communication protocols are necessary. A typical protocol stack for WSNs contains Physical, Data Link, Network, Transport and Application layers, and 3 management planes (Task, Mobility and Power) [15]. The stringent restrictions on energy consumption result in novel protocols for medium access, routing, transport, as well as applications, which sacrifice performance for energy efficiency. Ideally, the amount of time the transceiver spends in idle state and the communication overhead should be minimized in an attempt to maximize energy efficiency, especially in situations where the battery life is expected to last the entire life cycle of the application, which can be several years [15, 24]. Protocols used in Internet Protocol (IP) networks are not suitable for WSNs since energy consumption was not a critical factor when the standard was developed.

2.2.1 Physical Layer

The physical (PHY) layer deals with the communication specifications, such as frequency bands, data rate and modulation/demodulation techniques. Some of the tasks handled by the PHY layer include [25]:

- *Frequency allocation*: selection of a carrier frequency, typically from one of the Industrial, Scientific and Medical (ISM) bands.
- *Coding*: mapping of quantized bits to known symbol values, prior to modulation.
- *Modulation and Demodulation*: mapping of symbols into analogue waveforms prior to transmission and symbol recovery from waveforms at the receiver end.

Popular modulation techniques include phase shift keying (PSK), frequency shift keying (FSK) and amplitude shift keying (ASK).

2.2.2 Data Link Layer and Medium Access

In WSNs, most of the energy expenditure occurs during communication (which depends on whether the radio is on receive, transmit or idle state), and it has been shown to be as much as four times as energy expended in processing tasks [15]. Furthermore, significant energy is wasted due to overhearing, collisions, protocol overhead and idle listening. This has motivated significant research on MAC protocols to minimise the expended energy due to these phenomena. The data link layer (DLL) is responsible for ensuring reliable communication between sensor nodes and coordinating medium access. Tasks performed by the DLL include [15]:

- *Error control*: compensates effects of errors (caused by noise, interference and multipath) by using forward error correction (FEC) or Automatic Repeat request (ARQ) techniques to maintain reliable communication.
- *Medium Access control*: access to the communication medium by all network nodes is arbitrated through a MAC protocol located in the DLL.

MAC protocols can be broadly classified into contention-based protocols and schedule-based protocols.

2.2.2.1 Contention-based MAC Protocols

In contention based medium access, the transmitting node senses the channel (to determine if there already are on-going transmissions) before it transmits. An example is Carrier Sense Multiple Access with Collision Avoidance (CSMA-CA), where nodes only transmit if they sense the channel is idle. This is the scheme used in the IEEE 802.15.4 standard [26]. Various protocols have been developed to reduce collisions and maximize energy efficiency.

Sensor MAC (S-MAC) [27] is a synchronous duty cycle protocol. It has a divide message feature where messages are divided into frames, and transmitted sequentially when the

channel is seized by the transmitting node. S-MAC operates with a fixed-length periodic wake-up, sleep and listen scheme. However, it would be preferable to have an adaptive length scheme, as under high load conditions a fixed length scheme might not be appropriate.

Dynamic Sensor MAC (DS-MAC) [28] aims to reduce the latency in delay-sensitive applications by augmenting S-MAC with a dynamic duty cycle. Each node adapts its duty-cycle by keeping the listening period fixed and shortening its sleep period. To achieve this, nodes share their sleep-wake-up cycles and one-hop latency (i.e. difference between queuing and packet delivery) values with neighbour nodes, and they adjust duty cycles depending on the shared values.

Berkeley MAC (B-MAC) [29] addresses the idle listening issue by employing an adaptive preamble preceding any transmitted packet, eliminating the need for schedules. This preamble is used to alert the receiver of a transmission. Prior to transmission, the node waits a back-off period. In the case of a busy channel, the node waits for a second back-off period. If the channel is not busy, transmission takes place. The time it takes for the node to determine whether the channel is busy or not is equal to the preamble size. The duration for which the channel must be sensed for matches the preamble size so that the receiver has sufficient time to detect the preambles. Upper layers are responsible for changing the preamble duration accordingly, making B-MAC a very flexible protocol.

2.2.2.2 Schedule-based MAC Protocols

Schedule-based medium access is arbitrated through schedules which define time-slots where nodes can transmit in. All nodes have to be synchronised to the same time-base and schedules have to be shared amongst nodes in an efficient manner. These protocols are preferable to contention based schemes, as they avoid wasting energy by eliminating idle listening and collisions, and also introduce determinism into the network. However, one of the drawbacks of schedule-based schemes is the additional signalling overhead required to maintain the nodes synchronized.

An example of a schedule based protocol is Traffic Adaptive MAC (TRAMA) [30]. TRAMA operates with cycles consisting of a random-access period, followed by a schedule-access period. Nodes learn about their two-hop neighbourhood by capturing the neighbourhood information broadcast by other nodes during the random-access period. Nodes also periodically broadcast a list of receivers for the packets in their own queue to their neighbours. Using this information, nodes that should transmit/receive on the schedule-based period are allocated slots and the remaining nodes go to sleep.

2.2.3 Network Layer

There is an insurmountable amount of research done on routing protocols for WSNs [31, 32]. Simple approaches like flooding and gossiping were early energy efficient solutions to routing in WSNs, but several other protocols have since been developed to address the limitation of these basic routing schemes [31, 32]. However, for some applications, such as communication in industrial automation applications which are time-critical, the overhead introduced by more sophisticated routing protocols is prohibitive, and simpler routing approaches based on flooding are preferred [33].

In IP networks, the most popular routing metric is hop count. Low-power links in WSNs have been shown to be asymmetric and exhibit varying properties, making hop count unsuitable for WSNs [34]. Metrics which do not only reflect hop count, but also the link quality, are superior to hop count based metrics. Furthermore, since energy efficiency is critical in WSNs, routing metrics which reflect the remaining energy in sensor nodes are preferred.

The simplest approach to route data in a WSN is by flooding. In Flooding, the transmitting node broadcasts all packets to its neighbours, and all nodes re-broadcast all received packets, as illustrated in Figure 2.3. The main advantage of this scheme is that there is no communication overhead, since no routing paths have to be established and the data distribution is fast. However, this scheme is prone to implosion (caused by nodes receiving duplicated messages), and overlap (caused by two nodes in the same region sending similar

packets to the same node), and is a highly inefficient routing scheme due to the high energy consumption.

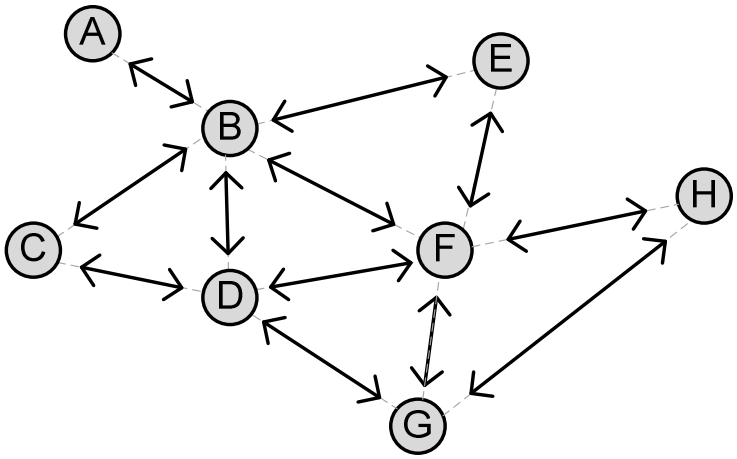

Figure 2.3: Flooding in WSNs.

To address the implosion issue in Flooding, an alternative routing scheme known as Gossiping has been proposed. Gossiping selects a single node for packet forwarding, and each node (upon receiving a packet) selects a single neighbour node arbitrarily to forward the received packet to. A disadvantage of this scheme over Flooding is latency since the packet distribution is slower.

Some nodes may consume more energy if they are repeatedly selected for data forwarding, especially the nodes closest to the sink. To counter this, some routing protocols for WSNs not only use metrics which consider the remaining energy in all nodes, but they also use clustering algorithms, such as Low Energy Adaptive Clustering Hierarchy (LEACH) [35], in an attempt to balance the network's remaining energy.

Routing in WSNs has been extensively investigated and numerous different methods have been proposed. These approaches are generally classified as Hierarchical routing, Geographic-based routing and quality of service (QoS) based routing [31, 32].

2.2.4 Transport and Application Layers

The transport and application layers have generally not received as much attention from the research community as the PHY, DLL and Network layers. The transport layer is responsible for [36]:

- *Congestion Control*: network reliability can be impaired under increased traffic so congestion control attempts to alleviate the effects caused by congestion.
- *End-to-end Reliability:* the Transport layer ensures that packets are delivered to their destination.

Several transport layer protocols exist [37], such as Pump Slowly Fetch Quickly (PSFQ) [38], which focuses on downstream reliability (i.e. sink to node) and proposes a hop-by-hop error recovery system where intermediate nodes keep track of the data they forward.

The application layer is responsible for source coding and data aggregation, amongst other functions. To minimize traffic in WSNs, data can be compressed. However, due to the resource constrained nature of WSNs, compression algorithms have to be modified such that their complexity is reduced. Also, especially in dense WSNs, data reported by sensor nodes is typically correlated. Therefore, source coding techniques can exploit this spatial/ temporal correlation.

2.3 WIRELESS SENSOR NETWORK STANDARDS

The *de facto* standard for WSNs is IEEE 802.15.4 [26]. Since its inception there have been amendments to augment the original standard to make it more suitable for a diverse set of applications and operating environments, and more recently other WSN standards have been proposed.

2.3.1 802.15.4 and ZigBee

IEEE 802.15.4 is a standard for low-rate wireless personal area networks (LR-WPAN). At the physical layer, 802.15.4 defines three carrier frequencies: 868 MHz, 914 MHz and 2.4 GHz, with 1, 10 and 16 channels, respectively, and data rates of 20 kbps, 40 kbps and 250 kbps [26]. 802.15.4 uses direct sequence spread spectrum (DSSS), a spreading technique

used to increase the frequency of a signal such that it occupies a much wider spectrum than the original information signal. This is achieved by combining data bits with pseudo-noise chips with higher data rate, making the wireless signal more robust to interference and jamming. It has been extensively used (and still is) in military applications since it has a low probability of detection and interception, as the power spectral density (PSD) is spread in frequency. DSSS in 802.15.4 at 2.4GHz, uses Orthogonal Quadrature Phase Shift Keying (OQPSK) where each 4-bit code is mapped to a 32-bit pseudo-noise chip [26]. For 868 MHz and 914 MHz, the information codes are mapped to 15-bit chips instead. Two node types are defined in 802.15.4:

- *Full Function Device (FFD)*: this type of node can act as a personal area network (PAN) coordinator, a simple coordinator or a device.
- *Reduced Function Device (RFD)*: this type of node only operates as a device.

In a practical network scenario, a star topology is used (with a FFD at the centre connected to RFDs as shown in Figure 2.4) but other topologies are supported. The FFD is responsible for managing the associated RFDs and exchanging data with them.

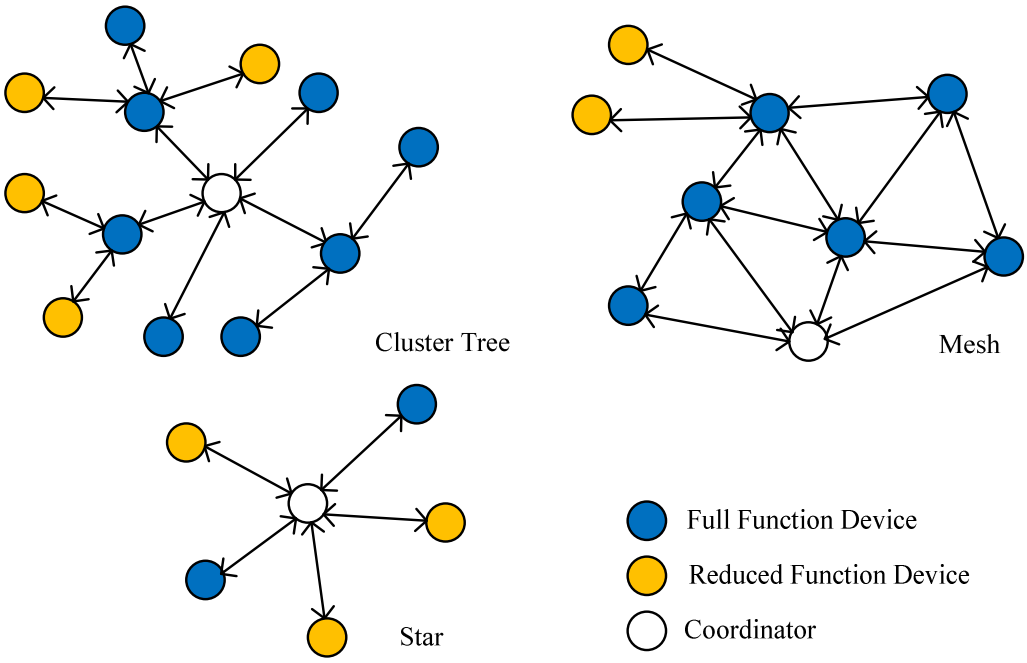

Figure 2.4: Topologies in ZigBee networks.

For medium access in beacon mode, 802.15.4 uses a super frame structure. This super frame structure defines a Contention Access Period (CAP) and a Contention Free Period (CFP) which consists of guaranteed time-slots (GTSs). In the CAP, any node can attempt to access the medium through slotted CSMA-CA, whilst in the CFP, the GTS is allocated to each node which requested the time-slot via the PAN coordinator, in such a way that nodes do not have to compete for channel access. Hence, for an 802.15.4 star network topology, the PAN coordinator dictates channel access and defines the super frame structure, where nodes can be put to sleep during the inactive period.

ZigBee is a popular wireless standard based on 802.15.4. Whilst 802.15.4 only defines the PHY and DLL layers, ZigBee extends its framework to the routing and applications layers. The fact that ZigBee networks function on a single static channel has an adverse impact on performance in the presence of interference or jamming. Therefore, frequency diversity schemes are preferable for harsh environments such as industrial scenarios.

2.3.2 WirelessHART and ISA100.11a

WirelessHART and ISA100.11a were developed for industrial applications and are based on 802.15.4. Although these are based on 802.15.4, there are some distinct differences between these technologies and ZigBee. WirelessHART (which is an extension of the wired HART protocol) and ISA 100.11a are both aimed at industrial applications, which are characterized by harsh environments where reliable communication is challenging. To counter the adverse effects of industrial environments, these standards adopt mesh networking, frequency hopping and time division multiple access (TDMA).

WirelessHART aims to achieve better communication reliability than ZigBee. Since a ZigBee network operates on one static channel during its lifetime, it is susceptible to static and multipath fading [39]. WirelessHART is based on the IEEE 802.15.4-2003 Standard, but specifies new Data Link, Network, Transportation and Application layers [39]. At the DLL, WirelessHART uses a Time-Synchronized Frequency Hopping protocol to combat static and multipath fading, and it employs TDMA for medium access, such that all devices are synchronized and communicate in pre-scheduled fixed time length slots.

WirelessHART uses Frequency Hopping Spread Spectrum (FHSS) to hop across 16 channels in order to mitigate adverse effects from interference. At the network layer, a mesh topology allows redundant paths, therefore increasing the network reliability at the cost of network latency and increased energy consumption.

WirelessHART is mainly designed to handle HART commands, whilst ISA supports HART, Profibus, Fieldbus Foundation and Modbus [40]. Additionally, there are some differences within the protocol stack, and each standard defines different device roles as well as different capabilities for each network device [40]. Furthermore, the time slot in WirelessHART is fixed at 10 ms, whilst in ISA 100.11a it is configurable [40]. Both standards support channel blacklisting to avoid channels with very high noise or interference. Table 2.2 highlights the differences and similarities between ZigBee, WirelessHART and ISA100.11a.

Table 2.2: ZigBee, WirelessHART and ISA100.11a comparison.

Standard	**ZigBee**	**WirelessHART**	**ISA100.11a**
PHY	IEEE 802.15.4 DSSS	IEEE 802.15.4 DSSS	IEEE 802.15.4 DSSS
MAC	CSMA-CA	Channel Hopping, TDMA, Channel Blacklisting	Channel Hopping, TDMA, CSMA, Hybrid Channel Blacklisting
Topology	Star, Cluster Tree, Mesh	Star, Mesh	Star, Mesh
Network Layer	AODV Routing Protocol	Graph and Source Routing	IPv6 Addressing (6LowPAN) based Routing

2.3.3 DASH7

DASH7 was initially a wireless technology for military applications [41]. In comparison to ZigBee, it differs in a number of aspects. The DASH7 Alliance Protocol (D7A) standard, based on ISO/IEC 18000 standard, defines communication in the 433 MHz band. In essence, it is based on active Radio-frequency Identification (RFID) technology such that devices using the D7A protocol stack can be extended to RFID devices, where tag-to-tag communication is possible, and the devices can be also used for non-RFID applications [42]. One of the features of D7A is the *Bursty, Light, Asynchronous, Stealth, Transitive* (BLAST) scheme which consists of sensing small data packets (less than 256 bytes) asynchronously, therefore eliminating the need for synchronization. BLAST stands for [43]:

- *Bursty*: data transfer is abrupt, and does not include video or audio.
- *Light*: packet size is limited to 256 bytes, and transmission of multiple consecutive packets is possible but is avoided.
- *Asynchronous*: no periodic hand-shaking or synchronization is needed between devices, as DASH7's main method of communication is by command-response.
- *Stealth*: no discovery beacons are used in DASH7, and end nodes can choose to respond only to pre-approved devices.
- *Transitive*: unlike other wireless technologies, DASH7 is upload-centric (and not download-centric) therefore devices do not need to be managed extensively by a fixed infrastructure (eg. base stations).

One of the advantages of using 433 MHz is the communication range: given the same output power, it enables much longer communication ranges than 2.4 GHz. This therefore eliminates, or alleviates, the need for multi-hop routing. However, even though the 433 MHz band is not as overcrowded as 2.4 GHz, there are some disadvantages. For example, channel hopping will not counter multipath propagation effects since the channel coherence bandwidth is larger than the whole 433 MHz band [42]. Table 2.3 highlights some differences between ZigBee and DASH7.

Table 2.3: Comparison of DASH7 and ZigBee (based on information from [43]).

Standard	**ZigBee (IEEE 802.15.4)**	**DASH7 (ISO 18000-7)**
Operating Frequency	868 MHz/ 915 MHz/ 2.4 GHz	433 MHz
Nominal Data Rate	250 Kbps	27.8 Kbps
Multi-hop Capabilities	Yes	2 hops only, extra hops can be added with RPL
Nominal Range (0 dBm)	75 m	250 m
Power	Rx: 84 mW, Tx: 72 mW	Rx: 7.5 mW, Tx: 31 mW

The protocol stack in D7A consists of the following: the application layer which describes the interaction between the application and communication layers; the presentation layer which defines the necessary data elements; the session layer which defines which events can trigger session initiation or scheduling; the transport layer which provides end-to-end communication services and is responsible for collision avoidance; and the network layer which hosts the Background Network Protocol responsible for group synchronization [42]. One of the main advantages of DASH7 over ZigBee is the reduced energy consumption as shown in Table 2.3. However, to the best of our knowledge, there is no complete open source DASH7 protocol stack available and therefore there are no results in literature to support the claims that DASH7 is indeed superior to ZigBee in terms of energy consumption, and whether the communication range can in fact span kilometres. Currently, the OSS-7 [44] open source DASH7 protocol stack is being developed, and it has support for basic communication between two nodes.

2.3.4 Other Wireless Communication Standards

To a certain extent, Wi-Fi (802.11) and Bluetooth (802.15.1) can also be used for WSNs. Wi-Fi, however, is significantly different from the other proposed standards because it was not designed for low power communication. Nevertheless, low power Wi-Fi transceivers have been recently introduced into the market, with examples such as GS1011 by

GainSpan [45] and CC3100/CC3200 transceivers by Texas instruments [46] readily enabling low-power connectivity to Wi-Fi networks.

2.4 APPLICATIONS

Generally, WSNs can be divided into two major categories: event detection WSNs and event monitoring WSNs, where data is only sent to a sink when an event is detected, and where data regarding a specific phenomenon is sent to a sink periodically, respectively. Various applications have been identified for WSNs. These include environmental monitoring, human health monitoring, structural health monitoring, industrial process monitoring and others. These applications are brought about by the ability of low cost sensing enabled by WSNs, as well as the ability of WSNs to be used in applications where it was previously unfeasible to install wired sensors. In industrial applications, for instance, some machinery with rotating components (such as motors) has previously gone un-instrumented because it was unfeasible to use cables [47].

Another example of monitoring which was previously unfeasible at low cost is habitat monitoring, where WSNs now allow the scientific community to model several aspects of wildlife. Table 2.4 lists various environments and examples of applications of WSNs.

Table 2.4: Examples of WSN applications.

Field	**Environment Characteristics**	**Applications**
Industrial Monitoring	Indoors, harsh	Condition monitoring, asset tracking, pipeline leak detection [48, 49]
Habitat Monitoring	Outdoors, possibly harsh	Wildlife species monitoring, localization and tracking [50, 51]
Environmental Monitoring	Outdoors, indoors	Gas, air pollution, sound pollution and water quality monitoring [52, 53]
Military	Outdoors, possibly harsh	Intruder detection and tracking, perimeter protection [54]

Health	Indoors	Patient tracking, non-intrusive vital signs monitoring [55, 56]
Agricultural	Outdoors, possibly harsh	Smart irrigation, precision agriculture [57]

In some of these applications, such as in agriculture, not all sensing takes place aboveground. For instance, in a precision agriculture system, monitoring the soil moisture is vital, and wireless sensor nodes buried in soil can replace wired sensors. To this end, WUSNs emerge as a potential solution for such applications, which in turn introduce unique challenges [8].

CHAPTER 3 WIRELESS UNDERGROUND SENSOR NETWORKS

3.1 INTRODUCTION

It is well known that the communication characteristics of WUSNs differ from traditional aboveground WSNs. This chapter introduces the concept of WUSNs and presents an overview of the different communication aspects applicable to WUSNs. A brief classification of WUSNs is presented and applications are identified. Propagation models and characteristics for the three communication channels are discussed.

3.2 WUSN CLASSIFICATION

Wireless Underground Sensor Networks are WSNs partially or totally deployed in underground environments. These networks are usually categorized as either WUSNs for mines and tunnels (which still use the wireless OTA channel for communication) and Soil Subsurface WUSNs, where a number of nodes are buried in soil and communicate wirelessly through soil with sink nodes located aboveground. Soil Subsurface WUSNs are further classified into Subsoil and Topsoil WUSNs, where the burial depth is more than 30 centimetres and less than 30 centimetres, respectively. Both Topsoil and Subsoil WUSNs can comprise underground-to-underground (UG2UG), aboveground-to-underground (AG2UG) and underground-to-aboveground (UG2AG) channels. WUSNs which contain all three channels are further classified as Hybrid Topsoil and Subsoil WUSNs [36].

Each category has its own set of challenges and WUSNs belonging to either category (i.e. WUSNs for mines/tunnels or Soil Subsurface WUSNs) differ since the communication medium is not the same. WUSNs are potential replacements for traditional WSNs in some applications [24, 36, 58] which currently use buried sensor nodes with a wired connection to the surface:

- *Landslide Prediction*: a Topsoil WUSN with nodes equipped with strain gauges can be used to monitor the movement of soil/dirt.

- *Volcano Monitoring*: buried sensors can be used to monitor volcano activity to alert entities of any hazardous conditions.
- *Structural Health Monitoring*: a wide variety of structural health monitoring applications in underground scenarios (such as sewers) can benefit from wireless connections.
- *Precision Agriculture*: the use of wires can interfere with irrigation activities, so a wireless solution for this kind of application is preferable.
- *Underground Pipeline Detection*: wireless sensor nodes deployed along a pipeline can enhance underground pipeline monitoring.

A typical WUSN deployment is illustrated in Figure 3.1.

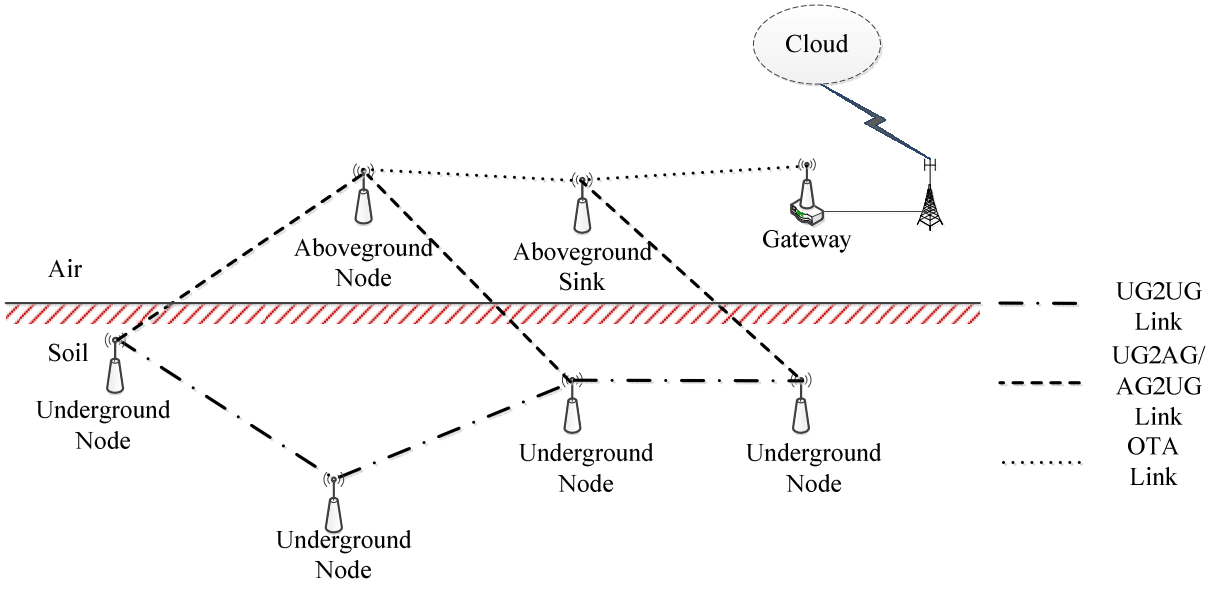

Figure 3.1: A WUSN for irrigation management.

3.3 WIRELESS PROPAGATION IN SOIL

Soil is mostly a mixture of organic matter, minerals and water. In comparison to OTA communication, wireless communication through soil faces various challenges. In air, environmental parameters such as temperature, humidity and wind velocity, have no strong effects on the communication quality, except for extremely high frequency (EHF) wireless communications, where atmospheric absorption, intense rain and snow can indeed affect

communication quality. OTA communications are typically more affected by the geometry of the surroundings, such as buildings and other obstructions which cause fading [59]. On the other hand, wireless communication in soil is sensitive to environmental conditions, and its performance is dependent on soil properties and conditions.

Figure 3.2 shows free space path losses for different centre frequencies for an OTA WSN link. For comparison purposes, Figure 3.3 shows the path losses for an underground link for two of the centre frequencies. It is evident that the path loss in the underground medium is much higher than OTA, as illustrated in Figure 3.3 for a underground-to-underground (i.e. both nodes are buried and communicate through soil) link with a volumetric water content (VWC) of 5%.

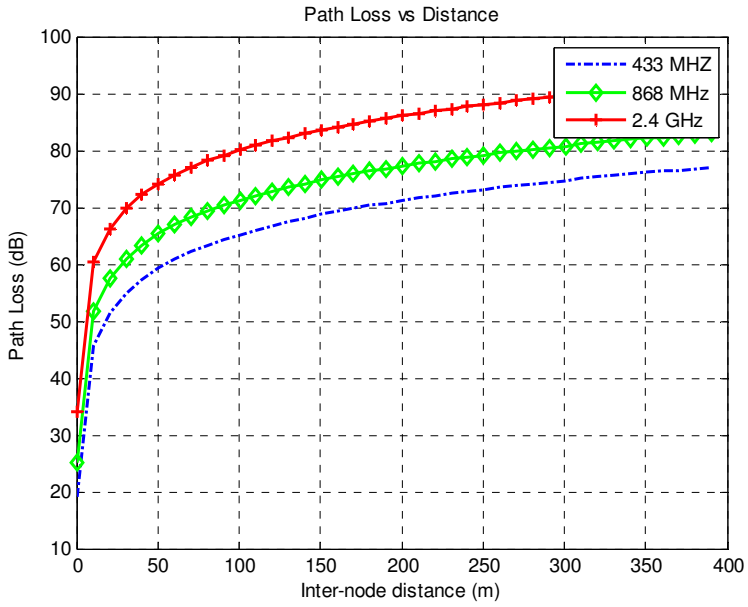

Figure 3.2: Path loss for OTA WSN.

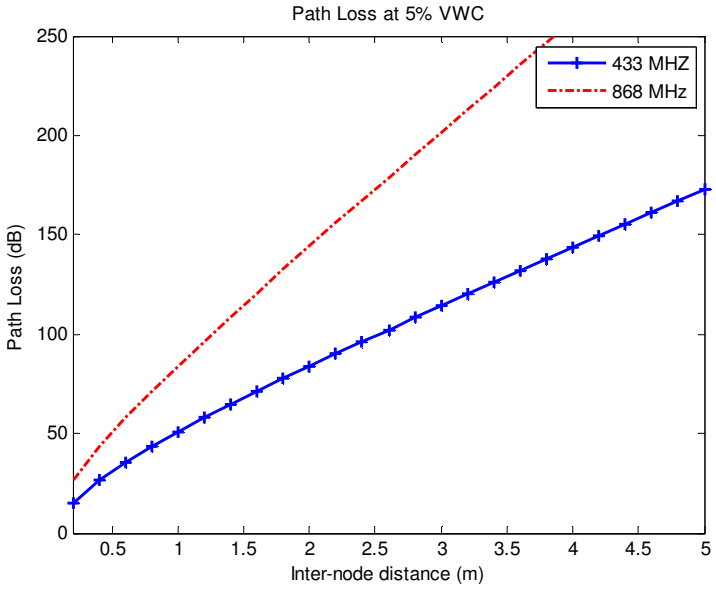

Figure 3.3: Path loss for WUSN with 5% VWC.

3.3.1 Soil Properties

The characteristics of EM propagation in a material are dependent on the conditions of said material, temperature, humidity, and other parameters which can ultimately affect the material's dielectric properties. Soil consists of free water, bound water, clay, sand, and also organic matter, and can be considered a dielectric. Dielectrics are characterized by their permittivity (ε), permeability (μ) and conductivity (σ) [60]. The relative permittivity (i.e. dielectric constant) of a material refers to the measure of resistance that is encountered when forming an electric field, with relation to the vacuum permittivity; permeability refers to the ability of the material to form a magnetic field within itself; and conductivity refers to the ability of the material to conduct an electric current [60]. The three properties mentioned above are all frequency dependent.

Properties such as soil density, soil texture, soil salinity and soil's VWC (which is a dimensionless ratio of water mass to the solid material in a given sample [61]) can affect the soil's permeability, permittivity and conductivity. For instance, sand is known to have relatively low conductivity and clay is known to have high conductivity [36]. High conductivity inherently results in more attenuation, so EM waves propagating in clayey

soil are subject to more attenuation than waves propagating in sandy soil. An increase in soil salinity has also been shown to cause an increase in path loss [62], and this can be caused by manure or fertilizers, or by the amount of salt in the irrigation water.

An increase in VWC increases the soil's relative permittivity [62], such that EM propagation in very wet soil is limited to short communication ranges. It is evident that propagation in soil is dominated by two aspects: the very high path loss, and the dependence on environmental conditions which affect soil conditions.

3.3.2 Modelling Wireless Propagation in Soil

To accurately determine, or predict, EM propagation characteristics based on soil conditions (and properties) an adequate model is necessary. Given the parameters previously mentioned, it is possible to model EM propagation in soil. Semi-empirical models such as Peplinski's model [63] have been proposed to estimate the soil's dielectric constant for frequencies in the 0.3 – 1.3 GHz band, by considering the sand percentage, clay percentage, VWC, soil particle specific density and soil bulk density, which can all be determined from analysing soil samples in a laboratory. Using these parameters, the real part of the complex permittivity, i.e. dielectric constant (ε_I), and tangent loss factor (ε_{II}) can be computed as [63]:

$$\varepsilon_I = 1.15\left[1+\frac{p_b}{p_s}\left(\varepsilon_s^{\alpha'}\right)+m_v^{\beta_{II}}\varepsilon_{f_w}^{I\alpha'}-m_v\right]^{\frac{1}{\alpha'}}-0.68 \tag{3.1}$$

$$\varepsilon_{II} = \left[m_v^{\beta_{II}}\varepsilon_{f_w}^{II\alpha'}\right]^{\frac{1}{\alpha'}} \tag{3.2}$$

where p_b is the specific density of soil particles, p_s is the soil bulk density, m_v is the soil's VWC, α^I is a constant, and β_I and β_{II} are empirically determined parameters from the soil's sand and clay percentages [63] as:

$$\beta_I = 1.2748+0.519S+0.152C \tag{3.3}$$

$$\beta_{II} = 1.3379-0.603S+0.166C \tag{3.4}$$

where S denotes the percentage of sand and C denotes the percentage of clay in the soil sample. The dielectric constant and tangent loss factor constitute the real and imaginary parts of the complex dielectric constant given by:

$$\varepsilon = \varepsilon_I + j\varepsilon_{II} \tag{3.5}$$

Given ε_I and ε_{II}, the attenuation constant (α) and phase constant (β), which constitute the real and imaginary parts of the propagation constant $\gamma = \alpha + j\beta$, can be computed as:

$$\alpha = 2\pi f \sqrt{\frac{\mu\varepsilon_I}{2}\left[\sqrt{1+\left(\frac{\varepsilon_{II}}{\varepsilon_I}\right)^2}-1\right]} \tag{3.6}$$

$$\beta = 2\pi f \sqrt{\frac{\mu\varepsilon_I}{2}\left[\sqrt{1+\left(\frac{\varepsilon_{II}}{\varepsilon_I}\right)^2}+1\right]} \tag{3.7}$$

where f is the operating frequency, and μ is the soil's magnetic permeability. The propagation constant is used to determine the propagation loss a wave experiences while propagating through a medium. Hence, it can be used to estimate the EM path loss in soil.

3.3.3 Impact of Soil on Propagation Characteristics

It is well known that the wavelength of an EM wave travelling in a material is dependent on the index of refraction of said material. Refraction has an impact on antenna selection as the wavelength in soil, or any other material with a different refractive index than that of air, has a different relationship with frequency (i.e. the refractive index is not 1). This means that an antenna designed for OTA communication will not radiate adequately when placed in another medium, since the relationship between frequency and wavelength is not the same as in OTA communication. The relationship between frequency and wavelength in soil is given by:

$$\lambda = \frac{c_0}{f\sqrt{\varepsilon_r}} \tag{3.8}$$

where c_0 is the speed of light in vacuum, ε_r is the soil's relative permittivity, f is the operating frequency and λ is the wavelength. It is evident that the wavelength reduces with

increasing permittivity. Furthermore, the wavelength λ at a specific frequency f changes in soil, since the wavelength is dependent on soil's permittivity which varies with VWC. Since the wavelength in soil changes with the soil conditions, an antenna which can accommodate a wide range of frequencies is necessary. This can be achieved with an ultra-wideband (UWB) antenna. As seen in Equation 3.8, a decrease in wavelength results in an increase in frequency, which means that in comparison to antennas for OTA wireless communication, the antenna size for WUSNs can be reduced.

The RSS is very sensitive to antenna positioning and at certain angles for the transmit and receive antennas, the RSS can be minimized for linearly polarized antennas due to cross-polarization. This effect can be reduced by using circular polarization, which is less sensitive to the receiver's and transmitter's relative positions. Additionally, because of the very high path loss in soil, efficient high gain antennas are necessary to counter-act the effect of the high path loss. The use of directional antennas can increase the range of the underground-to-aboveground channel by several meters as shown in [64]. Directional antennas have also been used for non-intrusive moisture sensing [65].

Additionally, refraction and reflection of signals cause multipath interference. In WUSNs, multipath can be caused by the presence of roots, stones or clay particles, and is therefore dependent on node location [66]. It is tempting to assume that nodes deployed at shallow burial depths result in better communication to aboveground nodes due to the shorter underground path length. This assumption is not always valid, as reflections at the soil-air interface can cause destructive interference, which is more severe in the case of very shallow depths. Both the antenna issue, as well as the reflection and refraction aspects have to be considered in WUSN deployment.

3.4 PROPAGATION MODELS

Communication in WUSNs takes place over three different channels: UG2UG, AG2UG and UG2AG.

3.4.1 UG2UG Channel

The UG2UG channel refers to the channel between two (or more) nodes buried in soil. The propagation model for this channel can be derived from a free space propagation model, with the inclusion of the attenuation effect caused by soil. The path loss (in dB) in soil is given by [66]:

$$P_{L1} = 6.4 + 20\log(d) + 20\log(\beta) + 8.69\alpha d \tag{3.9}$$

where d denotes the inter-node (i.e. between transmitter and receiver) distance, α is the attenuation constant (which describes the attenuation experienced by an EM wave propagating in a medium) and phase constant β (which describes the change in phase along the path travelled by the wave). This can be compared to a free space propagation model given by:

$$P_{L2} = -147.6 + 10\eta\log(d) + 20\log(f) \tag{3.10}$$

where η is the path loss exponent (whose value depends on the geometrical properties of the environment), f is the frequency and d is the inter-node distance.

Similar to the 2-ray ground model [59] for OTA communication, which considers reflections from the ground surface, communication in the UG2UG channel at sufficiently shallow depths experiences reflections at the soil-air interface. This effect, however, is not present for deep burial depths, as EM waves are attenuated to such an extent that the effect from reflections is negligible. Therefore, for shallow depths, where reflections occur, the path loss is given by [10]:

$$P_{L3} = P_{L1} - 10\log\left|1 + \frac{\Gamma d e^{\alpha\Delta r}}{(r_1 + r_2)} e^{-j\Delta\phi}\right|^2 \tag{3.11}$$

where Γ denotes the reflection coefficient; d denotes the inter-node distance; $\Delta r = (r_1 + r_2) - d$ corresponds to the difference between the reflected path and the direct path lengths; and $\Delta r = \left[2\pi(r_1 + r_2 - d)\right]/\lambda$ where λ is the wavelength in soil. Parameters r_1, r_2 and d are illustrated in Figure 3.4. The second term in Equation 3.11 refers to the reflected wave which can increase the RSS in the case of constructive interference, or

decrease it in the case of destructive interference. The reflected path is only possible if total internal reflection (TIR) takes place. This scenario occurs when the incidence angle at the soil-air interface is smaller than the critical angle. Figure 3.4 illustrates the direct path and the reflected path between a transmitter and receiver.

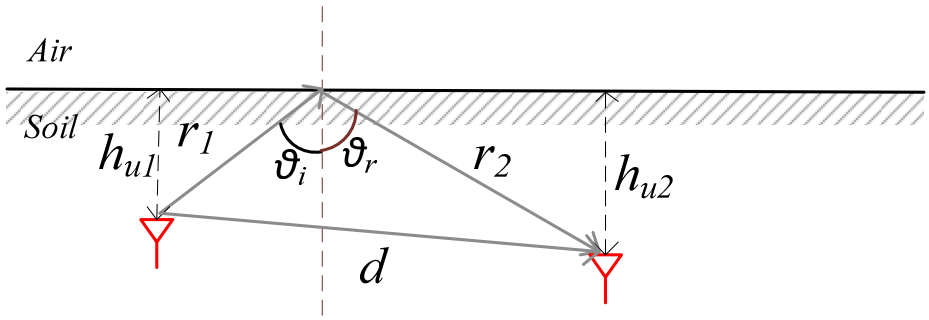

Figure 3.4: UG2UG Channel.

3.4.2 AG2UG and UG2AG Channels

Both AG2UG and UG2AG channels involve two media: soil and air. Apart from the path loss experienced by attenuation in soil and air, some transmission loss occurs at the soil-air and air-soil interfaces due to the difference in refractive indices of both media. Refraction is the change in direction of a wave caused by a medium change [59].

Snell's Law of Refraction can be used to compute the angle of transmission given the refractive indices of both media and the incidence angle. Snell's Law is given by [59]:

$$\frac{\sin\theta_1}{\sin\theta_2} = \frac{n_2}{n_1} \tag{3.12}$$

where a wave travels from a medium with refractive index n_1 to a medium with refractive index n_2 at an incident angle θ_1 and refraction angle θ_2. The refractive index can be computed based on the relative permittivity of a material as:

$$n = \sqrt{\mu_r \varepsilon_r} \approx \sqrt{\varepsilon_r} \tag{3.13}$$

where μ_r is approximately 1 for air and for most soils (which are typically non-magnetic). Based on Snell's law, Fresnel equations are used to compute the fraction of reflected and transmitted power for a wave crossing a medium interface. For oblique incidence, the reflectance R (which is the fraction of incident power that is reflected) is given by [59]:

$$R_{\parallel} = \left| \frac{n_1 \cos\theta_i - n_2 \cos\theta_t}{n_1 \cos\theta_i + n_2 \cos\theta_t} \right|^2 \tag{3.14}$$

$$R_{\perp} = \left| \frac{n_1 \cos\theta_t - n_2 \cos\theta_i}{n_1 \cos\theta_t + n_2 \cos\theta_i} \right|^2 \tag{3.15}$$

where $R_{\parallel}$ denotes parallel polarization, $R_{\perp}$ denotes perpendicular polarization and θ_i and θ_t are the incidence and transmission angles respectively. A negative Fresnel coefficient indicates that the incident wave has undergone a 180 degrees phase shift. The ratios of electric field magnitude can be computed as:

$$t_{\parallel} = \frac{2n_1 \cos\theta_i}{n_1 \cos\theta_t + n_2 \cos\theta_i} \tag{3.16}$$

$$t_{\perp} = \frac{2n_1 \cos\theta_i}{n_1 \cos\theta_i + n_2 \cos\theta_t} \tag{3.17}$$

If a wave travels from a medium where the refractive index is higher than the refractive index of the incident medium (such as in the case of soil to air), TIR occurs when the incidence angle is equal to the critical angle. The critical angle is determined using Snell's law by setting the transmission angle to 90 degrees.

The Brewster angle is the angle at which no reflection occurs and the incident wave is totally transmitted [59]. This is relevant for the UG2AG channel, where ideally no reflection should occur. On the other hand, the critical angle is important to the UG2UG channel, where ideally no transmittance should occur (i.e. ideally all power should be reflected) in order to maximize the RSS at the receiver. The path loss (in dB) for the UG2AG channel is given by [10]:

$$P_{UG2AG} = P_u + P_a + 10\log\left| \frac{1}{ve^{-j2\pi(d_1/\lambda + d_2/\lambda_0)}} \right|^2 \tag{3.18}$$

where P_u is the path loss in the underground portion of the channel, P_a is the path loss in the aboveground portion of the channel, v is the refraction coefficient from soil to air, λ_0 is the wavelength in free space, λ is the wavelength in soil and d_1 and d_2 are the underground and aboveground path lengths, respectively, as illustrated in Figure 3.5. The soil-air interface causes a transmission loss on waves propagating on the UG2AG channel.

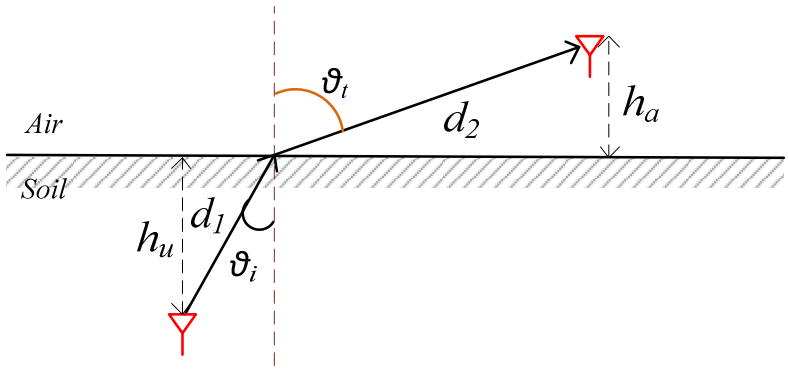

Figure 3.5: UG2AG Channel.

Similarly, the path loss (in dB) for the AG2UG channel is given by [10]:

$$P_{AG2UG} = P_u + P_a + 10\log\left|\frac{1}{ve^{-j2\pi(d_1/\lambda_0 + d_2/\lambda)}}\right|^2 \tag{3.19}$$

where P_u is the path loss in the underground portion of the channel, P_a is the path loss in the aboveground portion of the channel, v is the refraction coefficient from air to soil, λ_0 is the wavelength in free space, λ is the wavelength in soil and d_1 and d_2 are the aboveground path length and underground path length, respectively, as illustrated in Figure 3.6. In this case, since communication occurs from air to soil (i.e. from a medium with a small refractive index to a medium with a larger index), the transmission loss is higher than in the AG2UG channel.

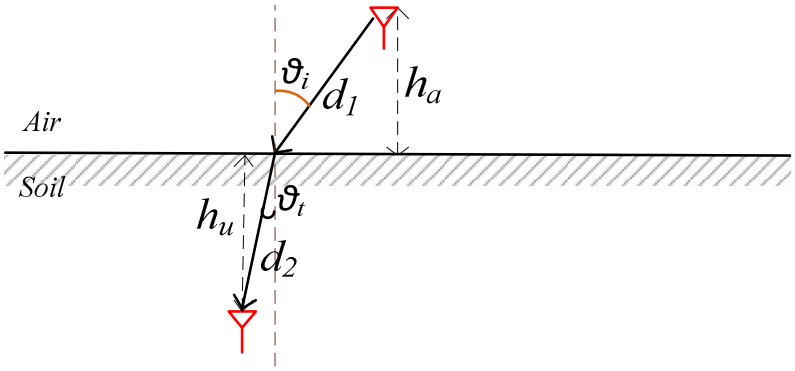

Figure 3.6: AG2UG Channel.

Therefore, a wave travelling from soil to air experiences three different losses: (severe) attenuation in soil; transmission loss at the soil-air boundary; and path loss in the OTA portion of the channel. The effect of refraction on waves travelling from one medium to another is an important aspect. It is possible that a highly refracted signal might not be detected by the receiver if the receiver is not correctly positioned in terms of height. Hence, in a UG2AG/UG2AG communication link, the height of the aboveground node and the burial depth of the underground node are very important considerations in deployment.

3.5 ALTERNATIVE COMMUNICATION APPROACHES

To address the very high path loss (see Figure 3.3) in the UG2UG channel, alternative communication techniques have been recently investigated. Magnetic Induction (MI) communication is a potential alternative to EM based wireless communication. The motivation for using MI based communication is the fact that soil's permeability is very similar to that of air [67], and the effects due to environmental conditions are minimal on MI performance. However, the rate of attenuation of MI is similar to EM, and at this stage significant research efforts are required for MI to achieve comparable performance to EM in terms of data rate. Additionally, MI communication links are inherently directional, since MI is very sensitive to coils' relative positions. Although recent research has focussed on increasing the capacity [68] and reducing effects of coil positioning and interference [69], the reported data rates are still very limited. Further investigation is necessary for MI communications to become an adequate replacement for EM based communication underground. The clear advantage of MI lies in the fact that passive (i.e. low cost) repeaters can be used, and the use of waveguides can significantly increase the transmission ranges while the same magnetic fields used for communication can also be used for wireless power transfer.

The sensitivity to coil positioning can be alleviated by using adaptive methods, such as the method employed in [70], where power transfer is optimized independent of coil orientation. From a wireless communication perspective, such a scheme can be used to create robust MI links invariable to coil position disturbances. On the other hand, MI is only applicable to UG2UG links, as it is not appropriate for UG2AG and AG2UG links

due to the high attenuation. Therefore, future deployments will probably integrate both EM and MI based solutions to leverage the advantages of each.

CHAPTER 4 LINK QUALITY ESTIMATION

4.1 INTRODUCTION

In this chapter, the concept of link quality estimation is introduced. Link quality estimation is discussed and the state-of-the-art is presented.

4.2 AN OVERVIEW OF LINK QUALITY ESTIMATION

LQE is a fundamental functional block of WSNs. Knowledge of the link quality is vital to select reliable forwarding links in routing, or to select stable links in topology management [15]. Selecting unreliable forwarding links can result in packet loss, which in turn incurs additional energy consumption due to packet re-transmissions. Hence, routing protocols which consider the link quality outperform conventional hop-count schemes. However, for LQE to be used effectively, an efficient way to estimate and characterize the link quality is necessary. LQE can be performed by various link quality estimators (or metrics), each with its own advantages and drawbacks [71].

4.2.1 Link Quality Modelling

For the theoretical study of link quality estimation, a basic model for low power link characteristics is required. The models introduced in [72] have been used in a wide range of WSN studies. The hardware noise floor (which is the noise present when no communication is taking place) is given by [72]:

$$P_n = (F+1)kT_oB \tag{4.1}$$

where F is the noise figure, k is Boltzmann's constant, T_0 is the ambient temperature and B is the transceiver's noise bandwidth. The signal-to-noise ratio (SNR) at the receiver is given by [72]:

$$SNR(d) = P_r(d) - P_n = P_t - L_x - P_n \tag{4.2}$$

where P_n denotes the noise floor, P_t denotes the transmit power, L_x denotes the total propagation loss, and d denotes the distance between receiver and transmitter.

The PRR can be statistically modelled directly from bit-error-rate (BER) probability. Assuming a frame length of N bits, the probability of receiving a frame in error is the same as the probability of getting one bit error. Hence, the PRR in terms of the packet error rate (PER) is given by:

$$PRR = 1 - PER = 1 - \left[1 - \left(1 - P_e\right)^N\right] = \left(1 - \frac{1}{2} e^{\frac{SNR(\mathrm{d})}{2}}\right)^N \tag{4.3}$$

where P_e is the theoretical BER probability for non-coherent FSK modulation [73]. The PRR depends on the modulation scheme, and formulas specific to other modulation schemes are listed in [73]. Figure 4.1 shows the theoretical BER for non-coherent FSK for frame lengths of 20, 50 and 127 bytes, and it is evident that shorter frame lengths result in better PRR for a given SNR.

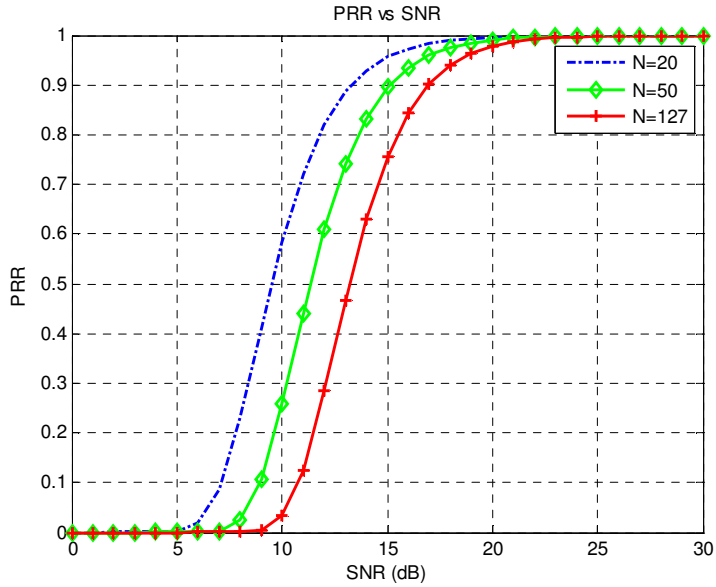

Figure 4.1: Packet Reception Ratio for frame lengths of 20, 50 and 127 bytes.

4.2.2 The Process of Link Quality Estimation

The process of LQE consists mainly of three steps [15]: link monitoring, link measurement and metric evaluation. Link monitoring consists of transmitting broadcast or unicast packets over a time window, also known as an estimation window. This can be accomplished either actively (by transmitting packets for the sole purpose of link quality

estimation) or passively (by opportunistically overhearing neighbour connections and considering all incoming traffic). The latter approach, although more energy efficient, is prone to erroneous estimation especially in low traffic WSNs because of the infrequent packet transmissions with random time differences. Link Measurement consists of collecting the appropriate data for metric computation. An example of link measurement is the collection of RSS for every received packet. Metric evaluation consists of taking the data collected in the Link Measurement step and computing a metric which represents the link quality.

The following properties are desirable in an estimator: precision, agility, stability and efficiency [15]. Precision refers to the ability of the estimator to provide meaningful estimates; agility refers to the ability of the estimator to detect changes in links; stability refers to the fact that the estimator should be immune to short fluctuations in the link; and efficiency refers to the fact that the memory required for the link statistics should be low, the complexity of estimation computations should be low and the estimator should be energy efficient (i.e. it should spend limited time collecting relevant statistics).

The low cost and low power nature of WSNs devices directly influences the link quality. Because of the non-perfect omni-directional properties of antennas, non-isotropic propagation affects the link quality, as the RSS varies with propagation direction [19]. Link quality estimators are generally classified as hardware based or software based estimators.

4.3 HARDWARE BASED LINK QUALITY ESTIMATORS

4.3.1 Received Signal Strength and Signal to Noise Ratio

The simplest, fastest and most ubiquitous estimator in low cost transceivers is RSS. RSS is typically computed over the first 8 symbols of received frames. Using the RSS as a LQE has a number of drawbacks. In the presence of interference, it is possible that the RSS is high, and therefore the link quality can be interpreted as high. Such a scenario can be caused by multipath, interference or signal variations introduced by the movement of

entities in the radio vicinity. In this scenario the actual signal may be even undetectable due to the corruption of the signal by interference. Nevertheless, the RSS is a desirable metric due to its simplicity and availability.

The SNR can also be used as a link quality metric. Similarly to RSS, SNR is based on the received power and is a hardware based estimator. For commercial-of-the-shelf (COTS) motes, obtaining the SNR is not as trivial as obtaining the RSS. One approach to obtain the SNR is to sample the RSS register prior to reception (i.e. sample the noise floor), and subsequently subtract the sampled noise floor upon a frame reception. In comparison to RSS, this metric is a superior estimator in high interference scenarios since it considers the noise floor.

4.3.2 Link Quality Indicator

Another hardware based metric is the LQI. Its computation varies between transceivers, and LQI is not available in all transceivers. For the CC2420 transceiver for instance, the LQI is computed as the average correlation value of the first eight received symbols in the preamble, and serves as an indicator of the chip error rate (CER) [74]. For the CC1101 transceiver, the LQI is a representation of the accumulated magnitude of the difference (i.e. error) between received symbols and ideal constellation symbols, over 64 symbols following the synchronization (SYNC) word [75]. LQI is typically not correlated with RSS. For instance, a weak signal received in noisy conditions can result in low RSS and low LQI, where as a received strong signal (compromised by constructive interference) can result in high RSS and low LQI, which ultimately indicates a poor link. Hence, a superior approach to using hardware estimators is to leverage their capabilities by combining them. LQI has been shown to have a very high variance, a property which has been successfully exploited for link selection [20], even though it requires a larger estimation window.

4.3.3 The Triangle Metric

The Triangle metric [76] is a hybrid estimator based on LQI, SNR and packet reception ratio (PRR). Using a combination of metrics is a better approach to using a single metric as hardware based estimators are typically biased (i.e. the RSS is only collected for received

packets therefore packet loss is not taken into account) [77]. By leveraging the ability of each of its constituent estimators to distinguish between different link qualities, this metric achieves finer granularity [76]. This metric exploits the fact that the mean LQI and mean SNR typically indicate a high quality link.

The Triangle metric is computed using a graph of the mean LQI against mean SNR. For a point **(*x*, *y*)**, where *x* denotes the mean SNR and *y* denotes the mean LQI (both averaged over *m* received packets), the link quality is computed as the Euclidean distance from the origin to this point. The PRR is embedded into the computation (so that packet loss information is also taken into account) by dividing both mean LQI and mean SNR by the number *n* of packets used to sample the channel [76]. The triangle metric is given by:

$$d_{\Delta} = \sqrt{\overline{SNR}_w^2 + \overline{LQI}_w^2} \tag{4.4}$$

where *w* denotes the estimation window width where both SNR and LQI are retrieved from *m* received packets.

The challenge with hardware based estimators is the limited access to low level information in COTS transceivers. For instance, BER or CER are good estimators [78], but these are not easily accessible in COTS hardware. As an alternative, BER and CER can be extrapolated from existing data in some cases.

4.4 SOFTWARE BASED LINK QUALITY ESTIMATORS

A fundamental drawback of hardware based estimators (one which the Triangle Metric attempts to address) is the absence of packet loss statistics in the estimates. For instance, a link with reasonable high RSS can still result in packet loss in the presence of interference. Software based methods consider packet statistics.

4.4.1 PRR

The simplest estimator which considers packet statistics is PRR. Considering *n* transmitted packets and *m* received packets over a link, the PRR for the link is given by:

$$PRR = \frac{m}{n} \tag{4.5}$$

Hence, the PRR ranges from 0 (i.e. no packets are received) to 1 (i.e. all packets are received). This is relevant because a high quality link will always have a high PRR (i.e. PRR is not ambiguous like RSS). Additionally, it has been shown that low power wireless links are asymmetric (i.e. PRRs for forward and reverse links differ by more than 10%) [72], so bi-directional PRRs can also be used to determine link asymmetry.

Another aspect is that PRR can be used to distinguish link connection regions. In [72], it was shown that low power links consist of three connection regions: connected (where the PRR is consistently above 0.9); transitional (where the PRR is between 0.1 and 0.9) and disconnected (where the PRR is below 0.1). In the connected region, links are mostly reliable and stable, but in the transitional and disconnected regions, the majority of links can be unreliable.

4.4.2 ETX

Expected Transmission Count (ETX) is an estimator that is able to detect link asymmetry by using bidirectional PRRs [34]. The ETX of a link is computed as the reciprocal of the product of forward and reverse delivery ratios, hence it provides an estimation of the bi-directional link quality:

$$ETX = \frac{1}{d_f d_r} \tag{4.6}$$

where d_f is the forward delivery ratio and d_r is the reverse delivery ratio. The d_r is computed as the link's PRR and the d_f is computed based on the number of received ACKs, which is indicative of the reverse PRR. The fact that bi-directional delivery ratios are included in the ETX computation means that ETX is able to detect asymmetry, which is mainly exhibited by links in the transitional region.

4.4.3 RNP

Number of packet retransmissions (RNP) [79], in contrast to ETX, RSS, LQI and PRR (which are all receiver-based estimators), is estimated at the transmitter, and it is computed

as the ratio of total transmitted and re-transmitted packets to the number of received packets, yielding an estimate of the total number of packet transmissions and re-transmissions required for a successful reception at the receiver. RNP has been shown to be a superior estimator in comparison to PRR, as PRR sometimes over estimates link quality for intermediate links, and RNP captures temporal aspects by taking time related packet loss information into account [79].

Hardware and software based estimators ultimately exhibit significant differences between them. In particular, some aspects to take into consideration are the facts that RSS can be high in the presence of interference, leading to an erroneous high link quality estimation for a link which might actually have low delivery ratios; LQI requires wide estimation windows due to its high variance; and PRR has less granularity over RSSI and PRR since it has to be estimated over a number of packets and not a single packet [80]. To address these drawbacks, several hybrid estimators have been proposed.

4.4.4 4-bit

An example of a hybrid software based estimator is 4-bit [81]. The 4-bit estimator uses 4 bits to represent information from multiple layers of the protocol stack. 1 bit is used to represent data from the PHY; the second bit is from the DLL and is used as an indicator of whether an ACK packet for a previously sent packet has been received; and the last two bits are used at the network layer to determine whether the route provided by a received packet is better than the available routes in the route cache.

4.4.5 F-LQE

Fuzzy Link Quality Estimator (F-LQE) [82] is a fuzzy logic based estimator with the following properties: it uses PRR to assess the channel's stability; it detects link asymmetry as the difference of the forward and reverse link delivery ratios; and it uses SNR to assess the channel quality. These metrics are all combined in a fuzzy logic approach to determine the overall link quality.

4.4.6 ETF

To address highly asymmetrical and therefore potentially unidirectional links, an estimator known as Expected number of transmissions over forward links (ETF) is proposed in [83]. In contrast to ETX which tends to favour links with similar forward and reverse delivery ratios, the ETF exploits highly asymmetric links [83]. For instance, a link with 50% -50% forward and reverse delivery ratios, is better for directional communication than a link with 75% -25% delivery ratios. However, the latter link might be preferable for one-way (i.e. uni-directional) communication, where a uni-directional link refers to a link with a 90% difference in PRR. An example of where this might be applicable is in data delivery to a sink in event-based WSNs, where using the ETF to select forwarding nodes can result in better packet delivery.

This scheme is implemented by relying on one hop neighbours with good bi-directional links to reference nodes, which can disseminate relevant link delivery ratio information by sending control packets to nodes which are unable to receive link quality information. Figure 4.2 illustrates some hardware and software based link quality estimators.

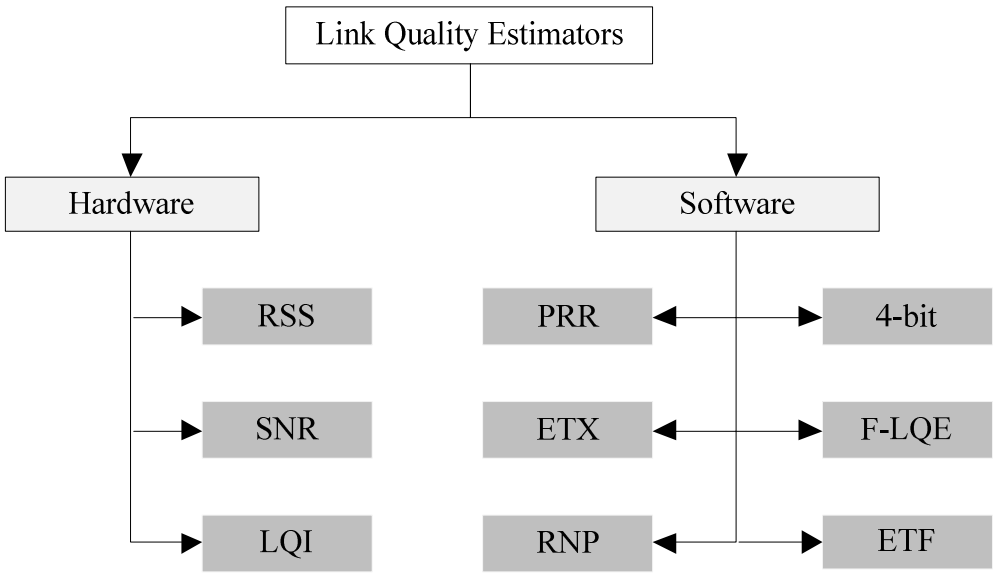

Figure 4.2: Hardware and software based estimators.

4.4.7 Interference Aware Metrics

In WSNs, two kinds of interference are prevalent: intra-flow and inter-flow interference. Inter-flow interference occurs between neighbouring nodes competing for the same busy channel and intra-flow interference occurs between nodes on the same path flow. Interference in WSNs adversely affects the link loss ratios and the link quality, hence it has to be identified and mitigated, and links affected by interference should be avoided. Interference aware metrics allow selection of links which have not been affected by interference.

iAware [84] captures effects of variation in loss link ratios, as well as intra-flow and inter-flow interference, and it is based on a combination of ETX, bandwidth and Signal-to-interference-plus-noise Ratio (SINR). MIC [85] is another interference aware metric which considers intra-flow and inter-flow interference. It is computed as a combination of the product of expected transmission time, number of interfering nodes, and the channel switching cost (CSC).

CHAPTER 5 DESCRIPTION OF EXPERIMENTS

5.1 INTRODUCTION

In this chapter, the experimental setup is presented. The first section describes simulations and the subsequent sections discuss the experimental protocol used for all measurement campaigns conducted at the University of Pretoria's Experimental Farm.

5.2 SIMULATION SETUP

A simulation to evaluate the PRR in the UG2UG channel was performed. This was motivated by the fact that a simulation allows a wide range of parameter choices which are not feasible to perform experimentally. The default propagation models on most network simulators are only applicable to OTA communication and are not suitable for underground simulations. To address this, an underground propagation model (such as the one presented in [66]) can be implemented in a network simulator by extending one of the built-in default propagation models.

5.2.1 Overview of Simulators

In network modelling, analytical approaches are usually unfeasible due to the fact that WSNs consist of a large number of network nodes with complex processes governing their behaviour. On the other hand, test-beds used in experimental investigations are costly to implement and maintain. Therefore, network simulators have emerged as an essential tool to analyse WSNs in realistic scenarios. The advantage of network simulators is that they abstract a number of lower layer level effects [86] and can be used to model virtually unlimited scenarios which are prohibitively costly if performed experimentally. Various network simulators are used in research on WSNs.

Network Simulator 2 (ns-2) [87] is the *de facto* network simulator. It is an object oriented discrete-event general purpose network simulator based on two languages: C++ for development and Object Tool Command language (OTcl) to setup and run simulations.

Although ns-2 is a very complete simulator, there is a steep learning curve involved before users can fully benefit from its features. Furthermore, ns-2 is mainly targeted at IP networks therefore a number of modifications to the source code are required to model WSNs. More recently, development has shifted towards ns-3 [88] which offers more features than ns-2.

Omnet++ [89] is also based on C++ and a scripting language. In contrast to ns-2, Omnet++ has a comprehensive graphical user interface (GUI). WSNs in Omnet++ can be modelled using the Mobility Framework which supports some MAC and other WSN protocols.

Castalia [90] is a simulator which is an extension of Omnet++ and is aimed specifically at wireless body area networks (WBANs). This makes it attractive over the former two simulators as the radio, propagation and protocol (PHY, MAC and Network) models are aimed at WSNs specifically. Although this simulator was initially aimed at WBANs, it is been extensively used for WSN simulations and there are a significant number of resources widely available to the research community.

Other simulators include Tossim [91], which is a system level simulator for TinyOS; Atmel Emulator (ATEMU) [92] which is an instruction level simulator for WSNs; and Avrora [93], a Java based simulator similar to Tossim with support for simulations at instruction level as well.

5.2.2 Simulation Details

Simulations to evaluate the PRR performance in UG2UG links were carried out in Castalia. ns-2 is mainly used for IP network modelling and modifications to the source code are required to perform WSN simulations. Other simulators such as Tossim, ATEMU and Avrora are aimed at instruction level simulations, and are system specific. Since our goal was not to perform system-level simulations, Castalia was selected as the simulator.

Castalia uses a log-normal shadowing model which is based on results from aboveground experiments. To simulate an underground (i.e. UG2UG) link, the underground path loss model in [9] was used. Peplinski's model [63] was used to set the soil conditions and properties which are necessary to determine the soil's dielectric constant.

The specification for the Texas Instruments CC1000 radio were input into Castalia. This was motivated by the fact that Peplinski's model is only valid for sub 1 GHz frequencies, hence 2.4 GHz cannot be used with this model. For this simulation, a number of nodes were placed around a circle (as illustrated in Figure 5.1) at various distances from the transmitter, which was placed at the centre of the circle. These receiving (i.e. destination) nodes were placed at 20 cm increments from 0 meters to 5 meters distances from the transmitter located at the centre.

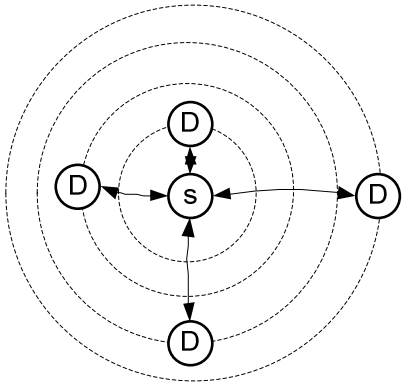

Figure 5.1: Node placement for 4 destination nodes.

Using a packet rate of 5 packets per second and a communication window of 3 minutes, 900 packets were transmitted for each inter-node distance, from the source (S) node to each destination (D) node. The PRR at each node was computed as the ratio of received packets over 900 packets for each D node. The reference distance for the propagation model was set as d_0 = 0.1 m, with a path loss of -52 dB. These values were selected from experimental data presented in [13]. The VWC was set to 5%. The simulation parameters are summarized in Table 5.1.

Table 5.1: Simulation parameters for Castalia.

Parameter	**Setting**
Volumetric Water Content	5%
Transceiver	TI CC1000
Frequency	433 MHz
Transmit Power	0 dBm
Packet Rate (per second)	5
Window width	180 seconds
Packet Size	100 bytes
Reference distance (path loss)	0.1 m (52 dB)

Figure 5.2 illustrates the interface between MATLAB (used to compute the soil parameters) and Castalia (used to perform the actual simulation).

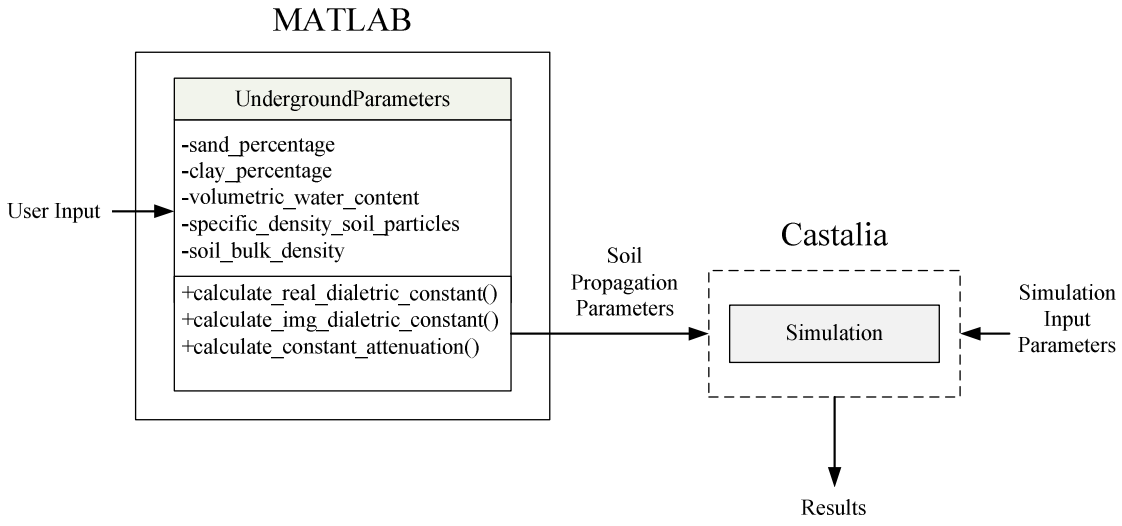

Figure 5.2: Interface between Castalia and MATLAB.

The simulation approach has a number of drawbacks. Most network simulators have limited capabilities in terms of antenna modelling and the main difference between traditional WSNs and WUSNs is the communication medium, where propagation properties differ. Additionally, refraction caused by the air-soil and soil-air interfaces in the

AG2UG and UG2AG channels, respectively, are complex to model due to soil irregularities and non-smooth surfaces. Therefore, this simulation is limited to the UG2UG channel only, and serves as motivation for the experimental investigation described in the remainder of this chapter.

5.3 EXPERIMENTAL SETUP

This section discusses all aspects regarding the experimental setup and protocol for all measurement campaigns conducted at the University of Pretoria's Experimental Farm.

5.3.1 Test-bed Configuration

The test-bed consists of three nodes: a source, a repeater (or relay) and a sink. The source serves as the source of the data packets; the relay acts as a repeater and forwards the received packets to the sink; and the sink receives all packets, and sends the packet data to a computer where the cyclic redundancy check (CRC) data, packet sequence numbers, LQI and RSS for all received packets are logged. The node (i.e. sink) connected to the PC acts as the communication coordinator (i.e. it is used to send a message to the source node to trigger the start of communication), and is the only node which is placed aboveground. The other two nodes (i.e. source and relay) are buried in soil and communication between them takes place over a UG2UG link. The communication links between the three nodes are illustrated in Figure 5.3. This configuration allows the test of communication links in all three channels (UG2UG, AG2UG and UG2AG) using a single setup.

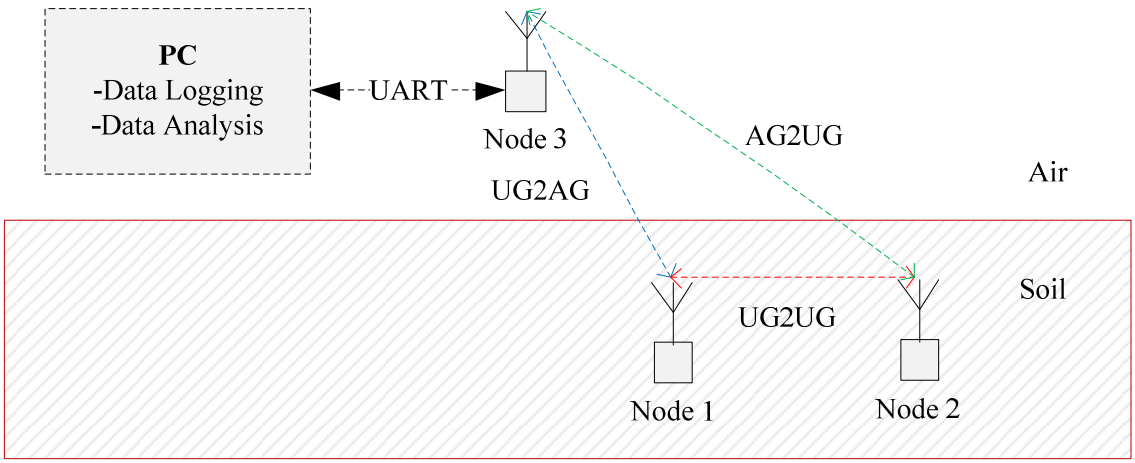

Figure 5.3: Test-bed configuration.

The experimental site is shown in Figure 5.4.

Figure 5.4: Experimental site at the Experimental Farm.

The topology of the holes used for burial of the source and relay nodes is illustrated in Figure 5.5. The topology was selected such that communication between any two nodes placed in any of the holes was not affected by other holes. These were setup such that UG2UG links with lengths of 40 cm, 80 cm, 125 cm, 200 cm and 250 cm could be tested. The motivation for this setup versus a conventional grid setup (as used in [14]) stems from the fact that holes in any UG2UG propagation path can influence the communication performance since the communication signal may cross multiple air-soil and soil-air interfaces. Therefore, this topology was selected in an attempt to eliminate this effect.

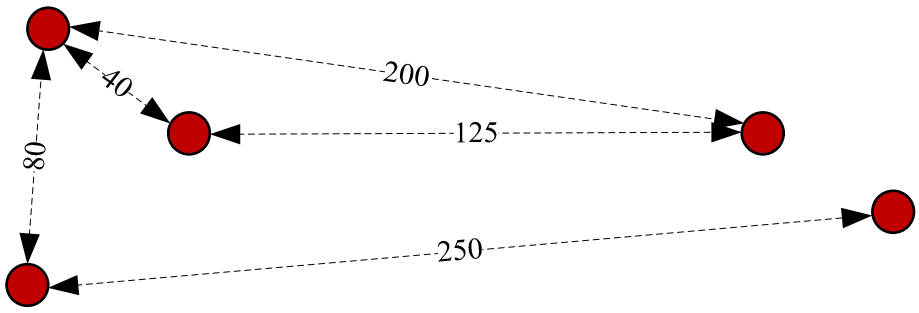

Figure 5.5: Hole topology for experiments.

5.3.2 Transceiver Configuration

The mote used for this investigation is the WizziMote [94], equipped with a Texas Instruments CC430 transceiver (which is based on the CC1101 transceiver). This node is

preferred over other popular motes (eg. TelosB) because it operates at 433 MHz, and this frequency has been shown to outperform 2.4GHz in underground deployments [62, 95]. However, one of the drawbacks of the WizziMote is the lack of TinyOS and Contiki support, making the transceiver configuration more time consuming. The configuration for the three transceivers is shown in Table 5.2.

Table 5.2: Transceiver configuration.

Parameter	**Setting**
Modulation	2-FSK
Data Rate	1.2 kbaud
Receiver Filter Bandwidth	58 KHz
Frequency Deviation	5.4 KHz
Centre Frequency	433 MHz
Transmit Power	10 dBm
Payload Length	30 bytes

Given the very high attenuation in soil, it is essential to configure the radio such that receiver sensitivity (and consequently communication range) is optimized. This can be achieved by correctly configuring the receiver filter bandwidth, frequency deviation, data rate, transmit power and packet length. The payload length is set to 30 bytes, which is long enough for most monitoring purposes in WUSNs. To maximize receiver sensitivity, 2-FSK was selected as the modulation format, instead of Gaussian FSK (GFSK). Although GFSK results in better spectrum efficiency, receiver sensitivity is more critical for these experiments. The settings in Table 5.2 used to maximize the receiver sensitivity were supplied by Texas Instruments.

5.3.3 Soil Characterization

As mentioned in Chapter 3, propagation characteristics are highly dependent on soil conditions and properties. Hence, it is necessary to characterize the soil properties before network deployment. To this end, four soil samples were collected at the experimental site.

The samples were collected for shallow (20 cm) and deep (40 cm) burial depths for both dry and wet soil conditions. A burial depth of more than 40 cm was not practically feasible because it was complex to retrieve buried nodes at deeper burial depths. Therefore, a maximum burial depth of 40 cm was selected. The samples were analysed for 4 parameters: sand percentage, silt percentage, clay percentage and VWC. According to Peplinski's model [63], these parameters are necessary to characterize the soil. All parameters were determined at the Soil Science's Laboratory at the University of Pretoria. The parameters used in the theoretical determination of the propagation parameters using Peplinski's model are included in Appendix A.

The soil's volumetric water content was determined using the oven drying method, which consisted of drying the soil for 24 hours in an oven at a temperature of 100 degrees Celsius. The VWC was determined by comparing the mass of the soil samples before and after the drying process as:

$$VWC(\%) = \left(\frac{wm - dm}{dm} \right).100 \tag{5.1}$$

where *dm* denotes the soil's dry mass and *wm* denotes the wet mass in grams. Table 5.3 shows the soil characteristics for all 4 samples.

Table 5.3: Soil sample analysis results.

Burial Depth	**Sand (%)**	**Silt (%)**	**Clay (%)**	**Dry VWC (%)**	**Wet VWC (%)**
20 cm	72.91	19	8.1	1.31	20.63
40 cm	58	33	8.9	10.85	22.25

5.3.4 Antenna Selection

Propagation in soil affects the antenna selection, since the relationship between wavelength and frequency of EM waves in soil is not the same as in free space. Soil's relative permittivity does not have a constant value, since varying moisture conditions effectively change the relative permittivity. The (dynamic) dielectric properties of soil cause the

wavelength of waves propagating in soil to either decrease or increase; therefore an antenna designed for OTA communication will not provide adequate propagation performance in varying soil conditions. To select the frequency bounds for an adequate antenna, the relative permittivity for all possible scenarios (i.e. different VWC, soil percentage and clay percentage) in Table 5.3 are computed. However, for the deployment in this chapter, the experiments are conducted only over a short period of time in two specific scenarios (i.e. there is no long term deployment which has to adapt to various conditions), therefore an antenna which accommodates the lower and upper bounds only can be selected, avoiding the use of an UWB antenna which is typically costly.

It is found that the best case (i.e. dry soil with the least amount of clay) and worst case (i.e. wet soil with the largest clay percentage) scenarios correspond to relative permittivity values of 5.24 and 19.3, respectively (computed using Equation 3.8). Given a frequency of 433 MHz, these relative permittivity values correspond to wavelengths of λ = 30.27 cm and λ = 15.77 cm respectively.

Antennas for OTA communications which correspond to these wavelengths have frequencies of 991 MHz and 1.9 GHz respectively. Since experiments were only conducted for the soil conditions given in Table 5.3, a dual-band Global System for Mobile Communications (GSM) antenna which covers these frequency bands was selected. Therefore, the buried nodes (i.e. the source and relay nodes) were equipped with dual-band GSM antennas, and the sink node was equipped with a 3 dBi 433 MHz antenna. A 433 MHz stubby antenna was also used to test the effect of selecting an appropriate antenna for the buried nodes. The RSS for a 40 cm UG2UG link was less than -85 dBm with the 433 MHz stubby antenna, whilst with a GSM antenna it was close to -62 dBm. Table 5.4 contains details on all antennas used in experiments.

Table 5.4: Specifications of antennas used in experiments.

Manufacturer	**Description**	**Freq. Bands (MHz)**	**Polarization**	**Length**
Taoglas	3 dBi Hinged Dipole	433.05–434.79	Vertical	198 mm
RF Solutions	0 dBi Quarter Wave Miniature Stubby 433 MHz Monopole	433	Vertical	48.12 mm
Unknown	2 dBi Dual Band GSM Antenna	880-960, 1710-1880	Vertical	120 mm

Using a GSM dual-band antenna (versus a UWB antenna) introduces some limitations. For optimal propagation, the antenna frequency has to be matched to the transceiver's centre frequency. Therefore, for frequencies which are not exactly matched to the communication centre frequency, there might be an increased path loss.

Another factor to consider is polarization. Assuming the same polarisation for both transmit and receive antennas, maximum RSS is achieved when the antennas are properly aligned to each other. A mis-alignment can result in polarization losses, reducing the RSS at the receiver. If two linearly polarized antennas have an orthogonal orientation relative to each other, the RSS at the receiver will be at a minimum. Although the antennas were positioned up right when placed in the holes during experiments, the force exerted by the sand when covering up the holes could have slightly misplaced the antennas. In [14] it was shown that the PER can be significant for large angle differences between the transmitter and receiver antennas. A linearly (i.e. vertical or horizontal) polarized antenna radiates in one plane. In circular polarization, the polarization plane rotates a full revolution at the rate of one wavelength, enabling communication links very robust to position changes. Therefore, circularly polarized UWB antennas are the optimal choice for WUSNs.

5.3.5 Experimental Protocol

On start-up, the sink (which is connected to the computer acting as a coordinator) sends a control message which is broadcast to the 2 buried nodes, instructing one of them to be the source node and the other to be the repeater. Both sensor nodes have built-in hard coded addresses, so on receipt of this control message, the node whose address matches the address in the address field of the received packet is set as the source node, and the node whose address does not match the address in the address field is set as the repeater.

To test the UG2UG forward and reverse links, the node which is instructed to be the source sets up its internal timer and starts transmitting packets continuously every 300 milliseconds, until the number of packets reaches 500. The relay node receives each packet, extracts the RSS and LQI of these received packets and appends them as a payload to new packets to be transmitted to the sink. These packets are then transmitted from the relay node to the sink node, where the RSS and LQI of the received packets, as well as the payload which contains the RSS and LQI of these packets received at the relay (where the RSS and LQI statistics in the payload correspond to the UG2UG link), are extracted. Therefore, the sink receives two packets per measurement: a packet from the direct transmission between the source and the sink, and a packet from the relay node. When testing the UG2UG channel, only the RSS and LQI information between source and relay is required, hence only the values in the payload of the relayed packet are logged, and the packet received from the direct transmission from the source is ignored. To test the reverse link statistics, a control message is sent so that the current relay becomes the source and the current source becomes the relay, effectively swapping the roles of the nodes and allowing the test of RSS and LQI for the reverse link.

To test both AG2UG and UG2AG links, only the sink and relay nodes are used. The sink configures a timer and transmits 500 packets at a 300 ms inter-packet interval. The relay receives these packets, extracts the RSS and LQI information, appends this information to the payload of a new packet, and transmits this new packet to the sink. The sink then extracts the received packets' LQI and RSS, which correspond to the UG2AG channel's

statistics, as well as the RSS and LQI in the payload, which corresponds to the RSS and LQI of the AG2UG channel.

Once all data has been collected, the temporal stability and other parameters can be statistically analysed. At the sink, the received packet's information is displayed on the serial terminal (via HyperTerminal) and logged to a file, whose contents are subsequently loaded into MATLAB, where the statistical analysis is performed. The sink and source nodes are shown in Figure 5.6. Although a deeper burial depth could be worth investigating, the available tools were only suitable to dig to 40 cm. For every link tested, the nodes were placed in the holes and then completely covered in soil. Although this method is more cumbersome, it results in a better representation of the UG2UG propagation characteristics, in contrast to previous work where nodes were placed in enclosures [9] and in paper pipes before burial [14], leading to scenarios which are not completely realistic (i.e. the communication is not strictly soil-to-soil). For the experiments performed in [9] and [14], where the authors were interested in evaluating the path loss, propagation through a paper pipe might only affect the RSS. However, link quality evaluation through a paper pipe might disrupt the properties of some parameters (eg. LQI) used in link quality estimation.

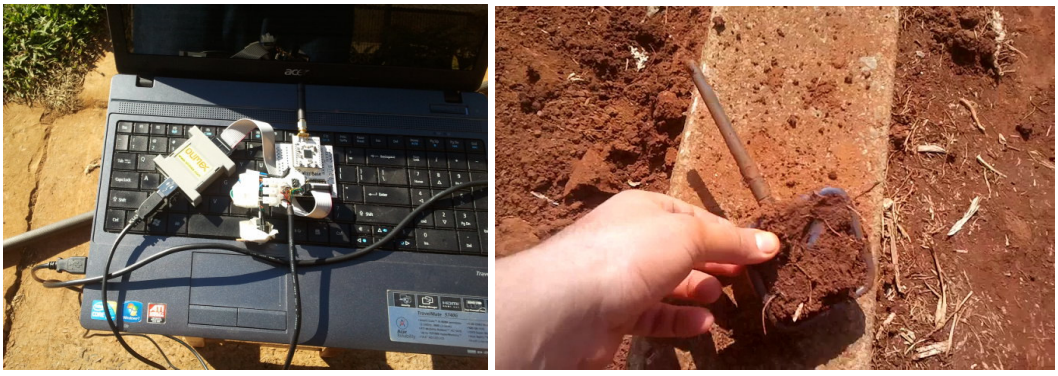

Figure 5.6: Sink node in a) and an unburied node in b).

5.3.6 Software Description

The flow diagrams below show the software running on the sink and source nodes. The flow diagram in Figure 5.7a) shows the software operation for the destination (i.e. sink) node, which is connected to a computer whose function is to display/log the relevant

packet data. The flow diagram in Figure 5.7b) shows the software running on the source node. Once all data has been logged, it is analysed off-line to extract the statistics of the desired parameters: RSS, LQI and PRR.

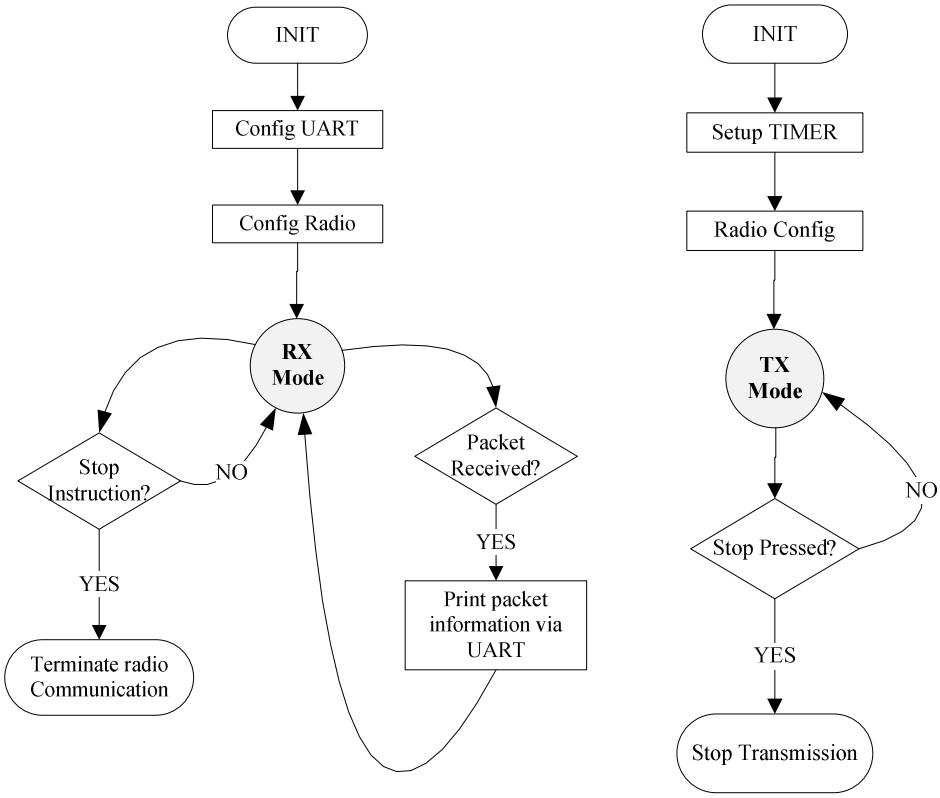

Figure 5.7: Software flow diagrams for sink and source nodes.

The relay (i.e. repeater node), which is not shown here, merely forwards the packets from the source to the sink, such that the statistics between the relay and source can be determined.

5.3.7 The AG2UG and UG2AG Test Protocol

When the AG2UG and UG2AG links are tested, the optimal height for the sink located aboveground has to be determined. According to [11], a transmitted wave travelling from soil to air is refracted and angularly defocused; therefore, there is typically an optimal height for the aboveground sink. For a burial depth of 20 cm and 40 cm, it was found that for the antenna configuration at the experimental site, the optimal height for the sink was around 1.2 meters (with a deviation of +/- 20 cm) for all position indices (i.e. horizontal

distances between transmitter and receiver of 1 to 10 meters) tested. The effect of antenna height on RSS is illustrated in Figure 5.8.

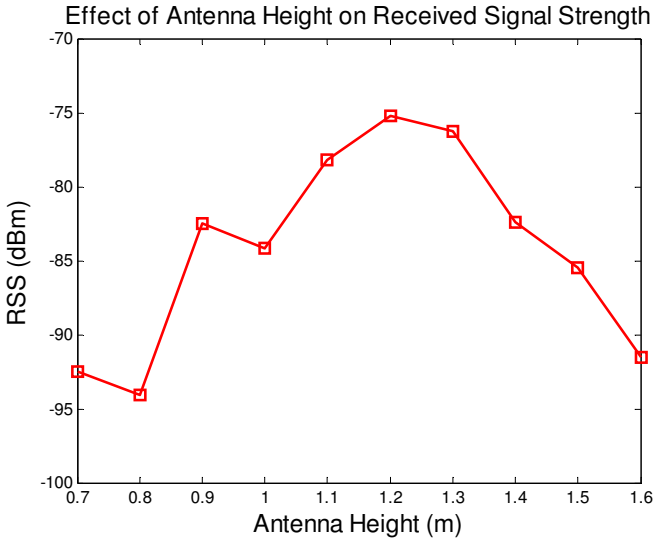

Figure 5.8: Effect of antenna height on RSS.

Hence, prior to each measurement, the sink node's height was appropriately adjusted. Figure 5.9 illustrates 2 position indices for the UG2AG and AG2UG testing scenarios.

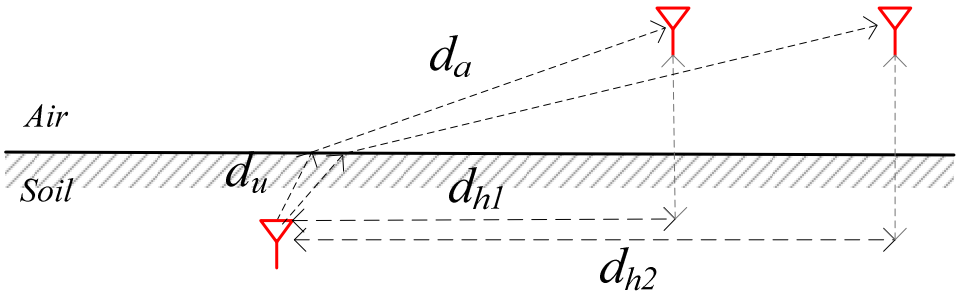

Figure 5.9: Testing scenario for UG2AG and UG2AG experiments.

It is noted that for all UG2AG/AG2UG experiments, the inter-node distance corresponds to the horizontal distance between nodes, as the direct inter-node distance cannot be easily determined due to the refraction at the medium interfaces. In Figure 5.9, d_{h1} and d_{h2} denote the horizontal inter-node distances for position indices 1 and 2, respectively, and d_u and d_a denote the distance travelled by the signal in soil and air, respectively, for position index 1.

The actual propagation distance between the buried node and the aboveground node is more than the horizontal distance. For instance, if the aboveground node is positioned at d_{h1}=5 meters and its height is 1.5 meters, and the underground node's burial depth is 40 cm, the communication distance is approximately 5.35 meters.

CHAPTER 6 RESULTS AND DISCUSSION

6.1 INTRODUCTION

This chapter contains details on the simulation and experimental results for all conducted experiments. All results are analysed and discussed.

6.2 SIMULATION RESULTS

The main drawback of the simulation approach is the absence of adequate models for temporal and spatial properties. Although the PRR can be analysed, link quality simulations cannot be performed without adequate spatial and temporal models. Figure 6.1 shows the PRR for a UG2UG link.

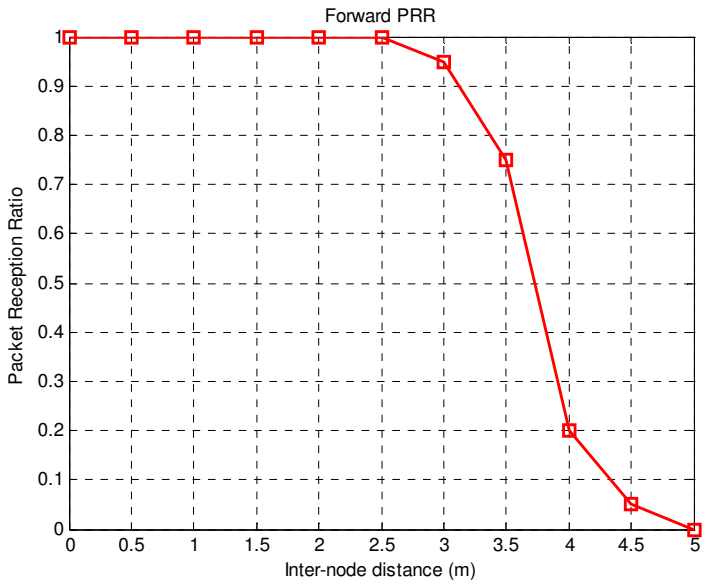

Figure 6.1: PRR vs inter-node distance for UG2UG link.

It is evident that the transitional region is narrow due to the limited communication range. The lack of comprehensive spatial and temporal models for WUSNs motivates the experimental analysis, which is discussed for the remainder of this chapter.

6.3 ABOVEGROUND EXPERIMENTAL RESULTS

Prior to underground link quality characterization, several tests to evaluate the link quality behaviour for the WizziMote in aboveground scenarios were conducted indoors and outdoors, in order to establish a basis for comparison with underground link characteristics. This was mainly done to determine link characteristics obtained from the transceivers, enabling a more educated interpretation of the results for the WUSN experiments.

6.3.1 Indoor Experiments

For the indoor scenario, the temporal characteristics for RSS and LQI were determined in an apartment, placing one node on a kitchen counter and two nodes in rooms, in a non-line-of-sight (NLOS) configuration (shown in Figure 6.2). The radio configuration for these experiments was the same as described in Table 5.2. The transmit (TX) mote was placed on top of a book shelf at 1.5 meters, and both receive (RX) motes were placed at 1.2 meters height.

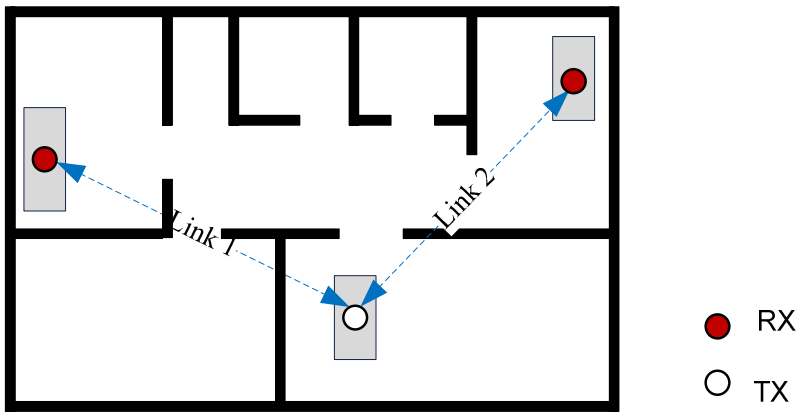

Figure 6.2: Indoor testing scenario.

It is noted that these were stationary environments (i.e. there were no moving entities) so the signal statistics might not be fully representative of an indoor environment such as an office with moving people, but they are representative of stationary conditions underground (i.e. there is no movement in soil) with static nodes. The RSS and LQI temporal characteristics for this experiment are shown in Figures 6.3 and 6.4.

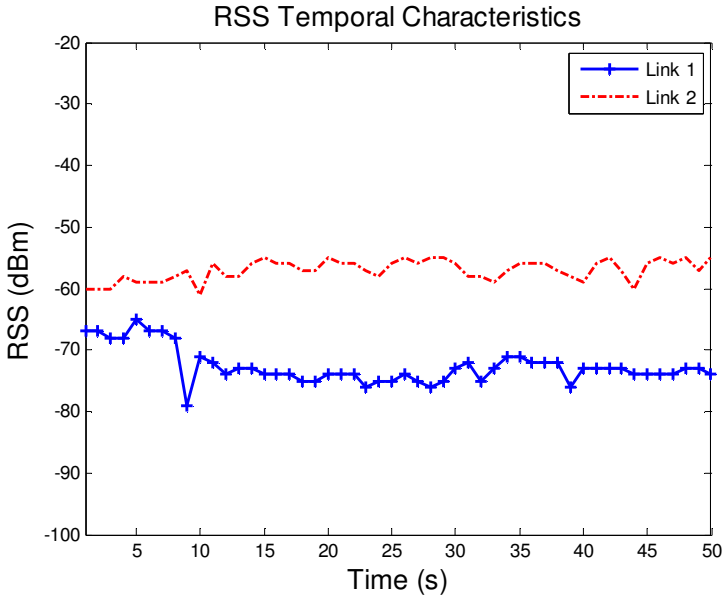

Figure 6.3: Indoor RSS temporal characteristics for links 1 and 2.

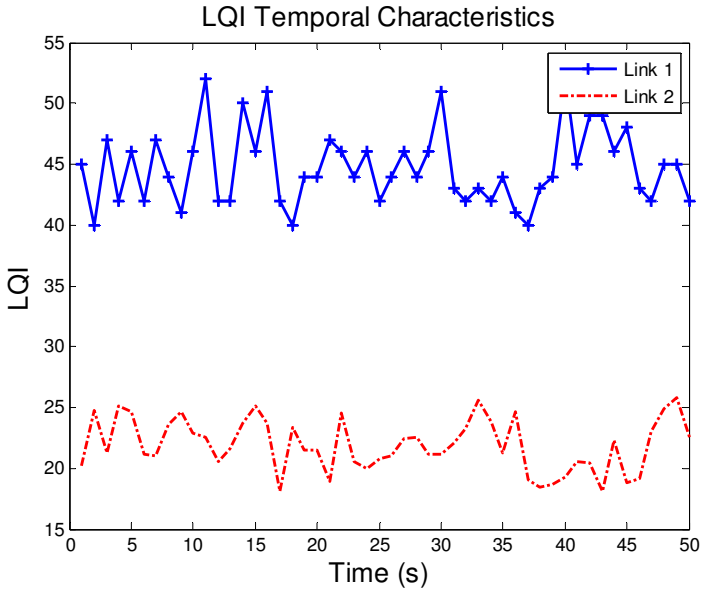

Figure 6.4: Indoor LQI temporal characteristics for links 1 and 2.

It is clearly seen that the LQI and RSS are relatively stable. The stability and low value of the LQI, in particular, indicates that the decoded symbols are very close to the ideal symbols, possibly because of the highly stationary nature of the testing environment. It is noted that the LQI reported by the CC430 transceiver has a minimum value of 0 (indicating best quality) and a maximum value of 127 (indicating worst quality). LQI

is expected to have a high variance [20]. The goal of these experiments is not to provide a comprehensive characterization of indoor links, but to provide a baseline for comparison of results with the underground experiments.

The difference between Link 1 and Link 2 statistics can be attributed to multipath effects. Only one wall obstructs the line-of-sight (LOS) path in Link 2, whilst 2 walls obstruct the path in Link 1. Therefore, the signal attenuation in Link 1 is slightly higher, and the LQI in Link 2 is expected to be better because the LQI for Link 1 is affected by multiple walls.

6.3.2 Outdoor Experiments

For the outdoors aboveground scenario, multiple links at the Experimental Farm were tested in LOS, with both nodes positioned at a height of 1.6 meters. The results for two links, at horizontal inter-node distances of 10 meters (Link 2) and 30 meters (Link 1) are shown in Figures 6.5 and 6.6.

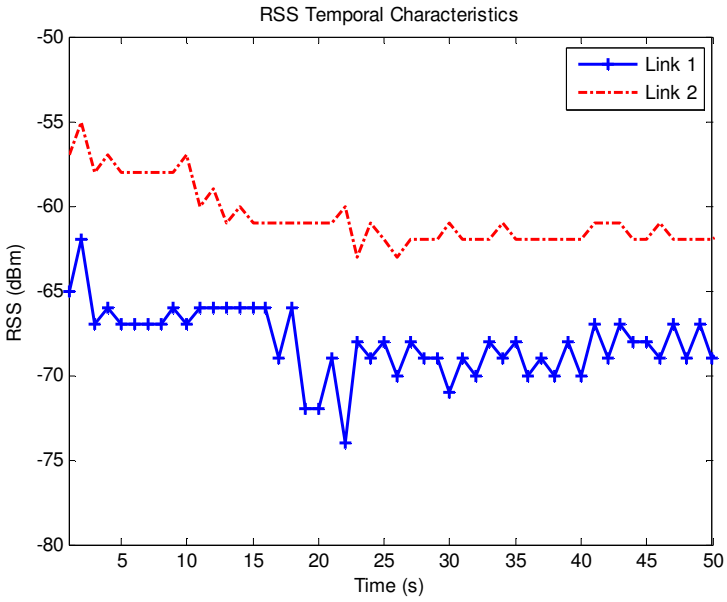

Figure 6.5: Outdoor RSS temporal characteristics.

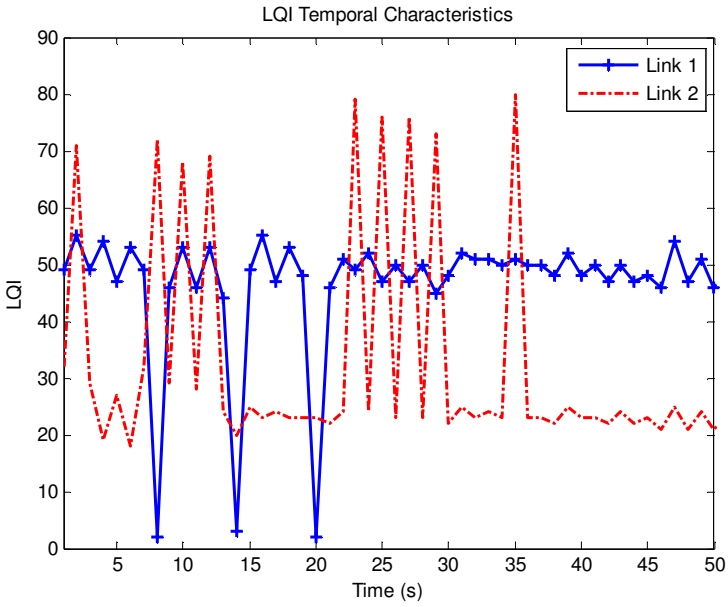

Figure 6.6: Outdoor LQI temporal characteristics.

The main difference between the indoor experiments and outdoors experiments is the absence of multipath effects due to obstructions, as there are no walls, and the communication links are strictly LOS. The LQI exhibits similar characteristics as indoors, with the exception of a few outliers, which can be attributed to moving entities around the experimental site.

6.4 UNDERGROUND-TO-UNDERGROUND RESULTS

6.4.1 RSS Temporal and Spatial Characteristics

The temporal and spatial characteristics of UG2UG links were determined for 5 horizontal inter-node distances (0.4 m, 0.8 m, 1.25 m, 2 m and 2.5 m) at two burial depths (20 cm and 40 cm). The temporal characteristics were determined over 500 samples (i.e. packets) and the spatial characteristics were obtained by averaging the RSS over the same number of packets. This procedure was performed at each of the five tested inter-node distances. The results are shown in Figures 6.7 and 6.8.

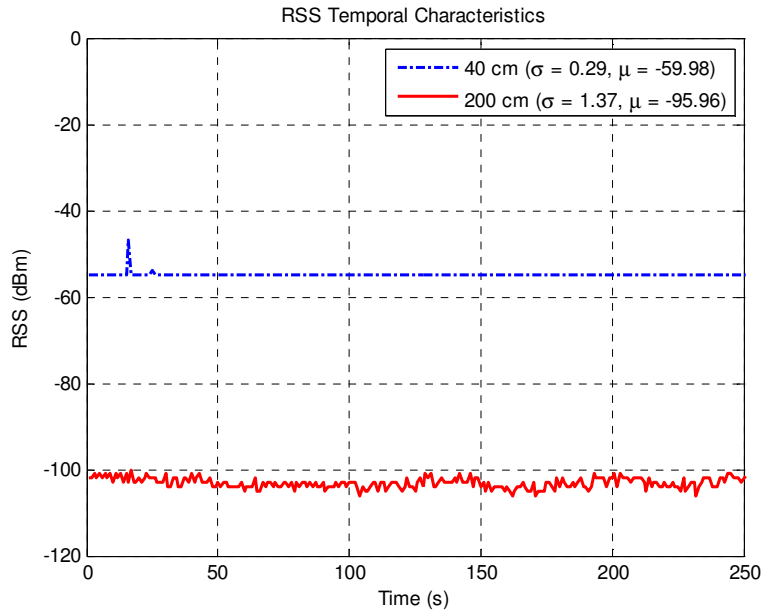

Figure 6.7: UG2UG RSS temporal characteristics.

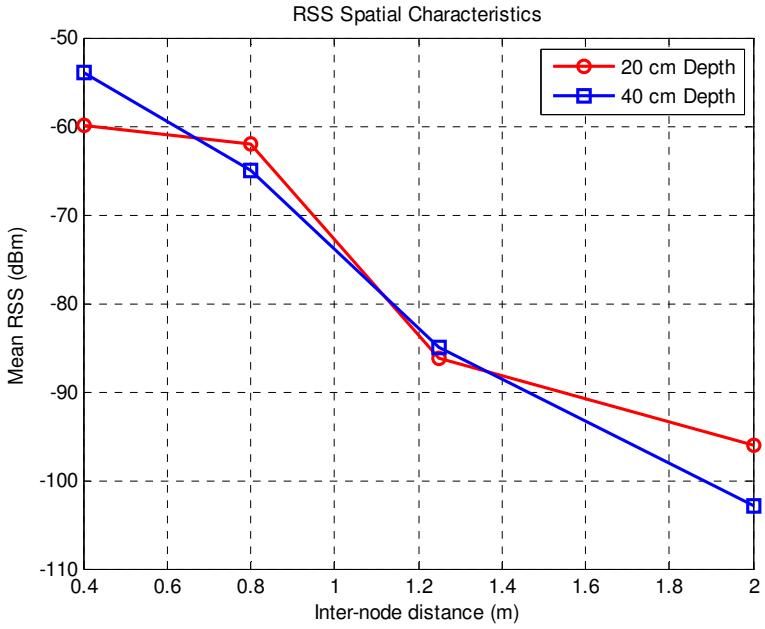

Figure 6.8: UG2UG RSS spatial characteristics.

In comparison to indoor and outdoor links (whose characteristics are shown in Table 6.1), it is clear that UG2UG links exhibit very high RSS temporal stability, with a variance of less than 1.5 dBm. It is noted that the higher RSS at a 40 cm burial depth can be attributed to an optimal burial depth (as suggested in [66]) since the effect of reflections from the

soil-air interface is reduced at larger burial depths, as the reflected signals are subject to severe attenuation and cannot be detected at the receiver.

Table 6.1: Typical RSS and LQI variance for 3 different environments.

Environment	RSS Variance	LQI Variance
Indoors	5.02	48.58
Outdoors	3.65	240.56
Underground	0.69	108.37

6.4.2 LQI Temporal and Spatial Characteristics

The LQI characteristics were measured over the same set of packets as the RSS characteristics. The temporal and spatial results are shown in Figures 6.9 and 6.10 respectively.

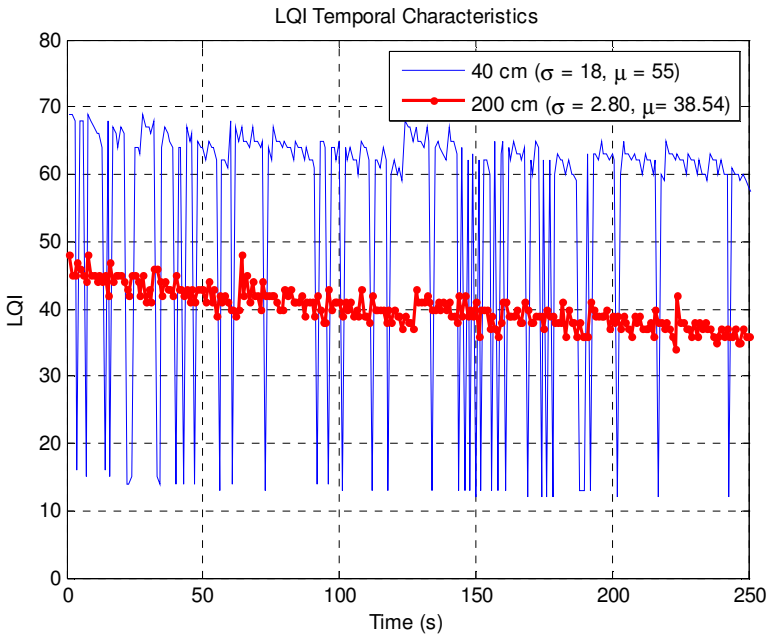

Figure 6.9: LQI temporal characteristics.

Since the LQI in the CC430 transceiver is based on the symbol error deviation (readers interested in more information are referred to [75]), it is reasonable to assume that the LQI

will be affected by interference. In a number of investigations reported in literature for OTA WSNs [20, 76, 80] LQI has consistently exhibited a high variance.

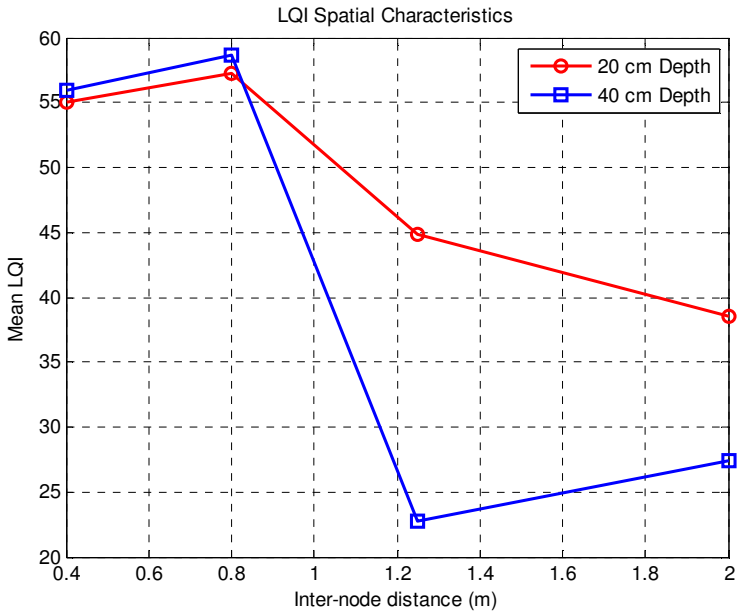

Figure 6.10: LQI spatial characteristics.

For UG2UG links, especially at a shallower depth, the reflection paths can constructively or destructively interfere with the direct UG2UG path, resulting in a lower LQI. At a deeper burial depth (i.e. 40 cm), these effects can be reduced and the LQI will consequently change. At longer inter-node distances, the effect of attenuation on reflected signals can result in a more stable LQI (i.e. smaller variance), and also result in a reduction in mean LQI (indicating higher quality) due to the absence of interference caused by reflected signals.

6.4.3 PRR and Link Asymmetry

The PRR for all tested UG2UG links is illustrated in Figure 6.11, where the link asymmetry is also shown. Link asymmetry is defined as the difference between the PRRs of the forward and reverse links [96]:

$$\left| PRR_{ij} - PRR_{ji} \right| \tag{6.1}$$

where PRR_{ij} is the PRR for the link between nodes i and j, and PRR_{ji} is the PRR for the link between nodes j and i. The larger the difference between the PRRs, the more asymmetric the link is.

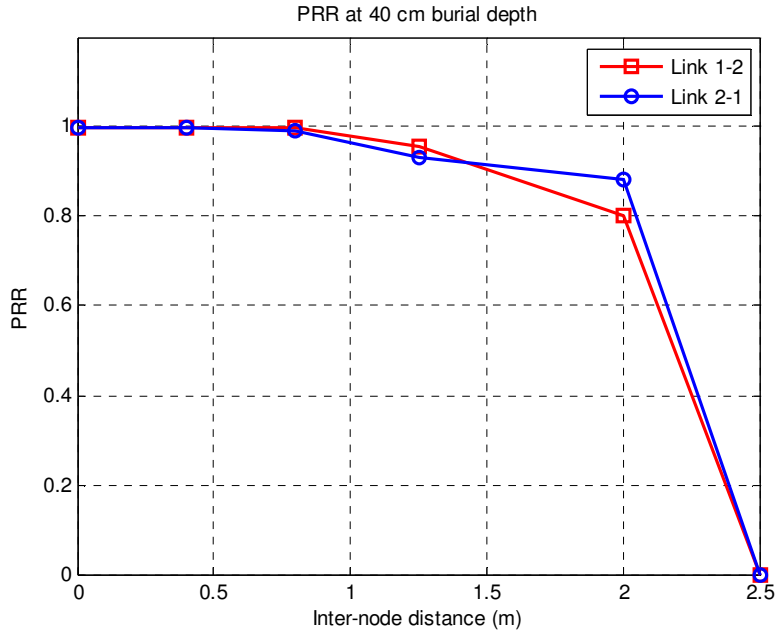

Figure 6.11: Forward and reverse PRRs for UG2UG links.

In WSNs, three communication region regions exist: connected, transitional and disconnected [72]. The connection region is the region where the PRR is above 0.9; the transitional region of a link is the region where the PRR is between 0.1 and 0.9; and the disconnected region is where the PRR is less than 0.1. For both forward and reverse links tested, the transitional region (illustrated in Figure 6.11) is between 1.5 and 2.4 meters, which corresponds to a 36% of the total communication range (i.e. 2.5 meters). The connected region (between 0 and 1.5 meters) is larger than the transitional region, and the disconnected region is extremely narrow. The asymmetries for all the tested links are shown in Table 6.2.

Table 6.2: Asymmetry for the UG2UG channel.

Inter-Node Distance (m)	0.4	0.8	1.25	2.00
Asymmetry	0	0.009	0.0250	0.0820

It is evident that UG2UG links are very symmetric. This has fundamental effects on link quality estimation, as discussed in Chapter 7.

6.4.4 RSS, LQI and PRR in Wet Scenario

Considering the theoretical background presented in Chapter 3, an increase in VWC results in higher path loss. Previous studies have shown a difference of up to 12 dBm for a 7% VWC increase [13]. However, in [13], the effect of moisture on the signal's wavelength was not taken into account and it is reasonable to assume that under the same soil conditions the path loss could have been reduced if a proper antenna had been selected. The experimental results for the wet UG2UG scenario were only obtained at inter-node distances of 0.8 and 2 meters at a depth of 20 cm, since it was impractical to test at a depth of 40 cm, as retrieving the nodes after experiments proved to be very challenging in muddy conditions. A comparison of the RSS characteristics in dry and wet scenarios is shown in Table 6.3.

Table 6.3: Comparison of RSS for wet and dry scenarios.

Inter-node distance (m)	RSS Mean (Wet)	RSS Standard Deviation (Wet)	RSS Mean (Dry)	RSS Standard Deviation (Dry)
0.8	-65.8	0	-61.99	0.09
2	-103.8	0.084	-95.96	1.37

These results show that at 0.8 m there was an increase in attenuation of 3.81 dBm and 7.83 dBm at 2 meters. However, no significant changes were observed for LQI. LQI exhibited similar temporal and spatial behaviour as in the dry scenario. PRR was reduced as the added attenuation resulted in the RSS at 2 meters to be very close to the receiver sensitivity, thereby increasing the PER, consequently decreasing the PRR.

6.5 UNDERGROUND-TO-ABOVEGROUND AND ABOVEGROUND-TO-UNDERGROUND RESULTS

In comparison to the UG2UG channel, there are some distinct differences in AG2UG/UG2AG channels. Firstly, an EM wave has to transverse two media (i.e. air and

soil), where the medium boundaries affect propagation characteristics [60]. It is known that a wave travelling from soil to air undergoes angular defocus [11]. Secondly, the attenuation experienced at the medium interfaces (i.e. air-to-soil and soil-to-air) differs due to the different refraction angles at each medium, as well as the different refractive indices whose values are dependent on the VWC.

6.5.1 RSS Temporal and Spatial Characteristics

The temporal statistics shown in Figure 6.12 were obtained at 4 meters inter-node distance. These statistics are comparable to OTA WSNs. Such a result is expected because the temporal variation introduced by the underground portion of the channel is very small, therefore the temporal characteristics of the OTA portion of the channel dominate. It is noted that the inter-node distances in the AG2UG and UG2AG experiments denote horizontal distances (as illustrated in Figure 5.9) since signals in these channels do not travel in a straight path due to refraction at the medium boundaries.

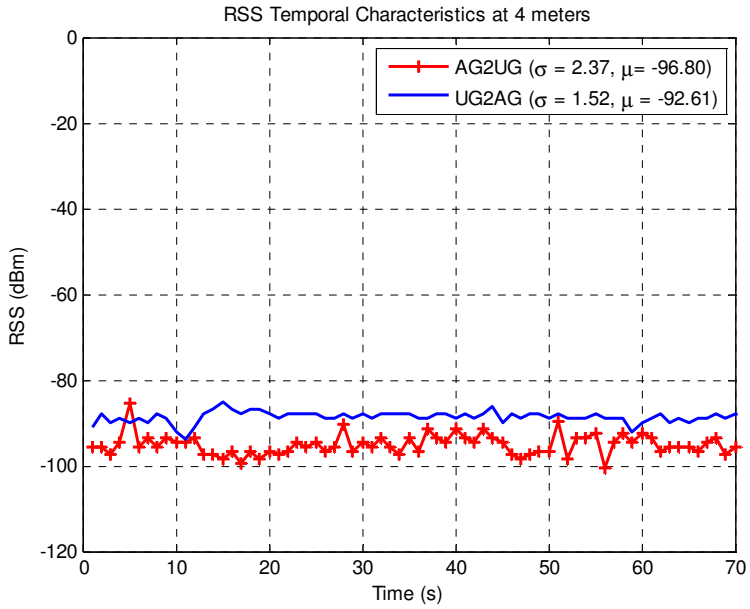

Figure 6.12: AG2UG/UG2AG RSS temporal characteristics.

The transmission losses at the air-soil interface are larger than the transmission losses at the soil-air interface, as soil's refractive index is larger than that of air. Therefore, the communication range for the AG2UG channel is smaller, as shown in Figure 6.13.

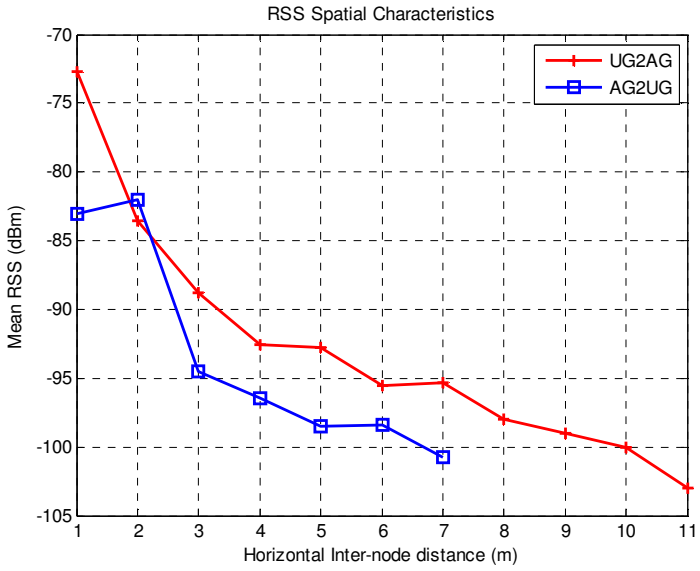

Figure 6.13: AG2UG/UG2AG RSS spatial characteristics.

6.5.2 LQI Temporal and Spatial Characteristics

The LQI behaviour for the AG2UG and UG2AG links differs from the behaviour observed in UG2UG links. The temporal characteristics are shown in Figure 6.14. It is seen that the LQI for AG2UG/UG2AG links in general has lower variance then the LQI for UG2UG links, as illustrated in Figure 6.14.

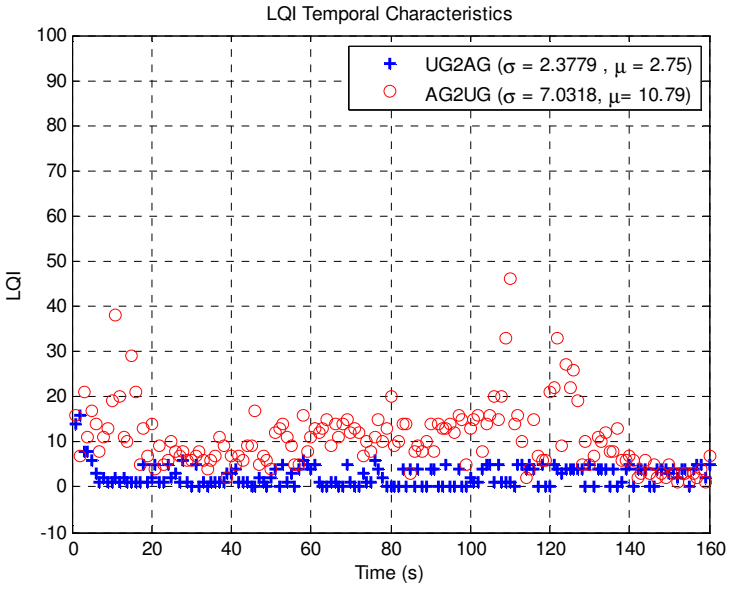

Figure 6.14: AG2UG/UG2AG LQI temporal characteristics for 1 meter.

Regarding the spatial characteristics, whereas in UG2UG links the mean LQI decreases with increasing distance, this behaviour is not observed in UG2AG/AG2UG links (shown in Figure 6.15). This is possibly due to the fact that an interfering path from the UG2UG channel does not exist, as communication is strictly between underground and aboveground nodes.

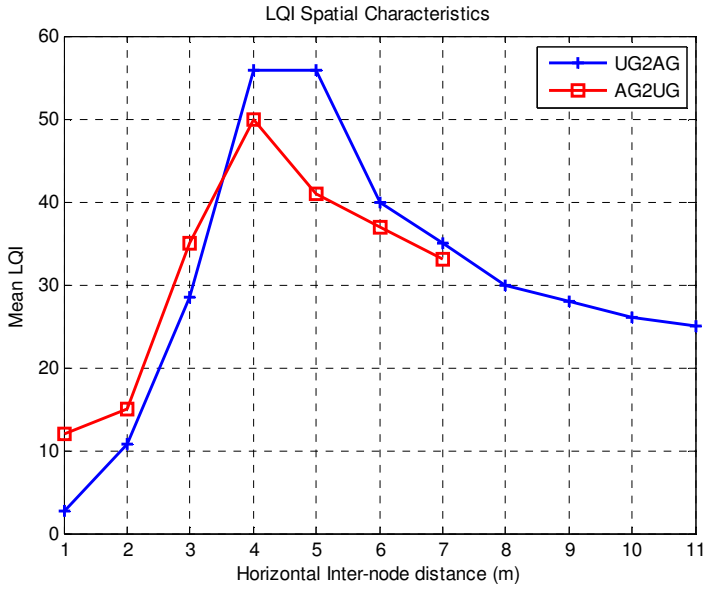

Figure 6.15: AG2UG/UG2AG LQI spatial characteristics.

The LQI is affected by refraction, reflection and angular defocus at the medium interfaces. Further modelling and experimentation is required to determine the exact effect of these propagation phenomena on LQI.

6.5.3 PRR and Link Asymmetry

Links in the AG2UG and UG2AG channels are generally not symmetrical. This lack of symmetry is illustrated in Figure 6.16.

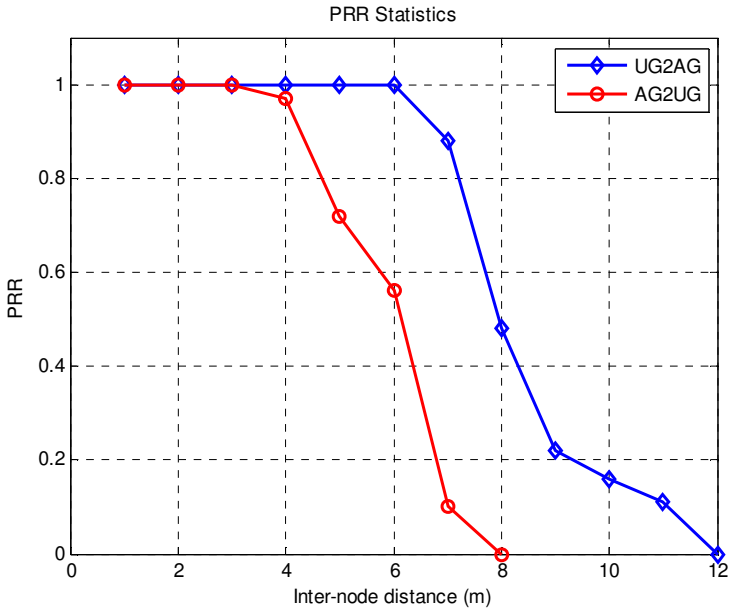

Figure 6.16: PRR for UG2AG and AG2UG links.

This shows that although the transitional regions for both channels have similar width (relative to their total communication ranges), the connected region of the AG2UG channel is smaller due to the smaller communication range. As the signal is reflected and attenuated at the air-soil interface, the RSS drops to values close to the receiver sensitivity, therefore decreasing the PRR. A pair-wise comparison between the links was conducted up to 7 meters, at which point the AG2UG channel reached its maximum communication range. The asymmetry ranges from 0 (where both links still have a PRR of 100%) to 0.78. Table 6.4 shows the asymmetry values for these links.

Table 6.4: Asymmetry for UG2AG and AG2UG links.

Horizontal Inter-node distance (m)	1	2	3	4	5	6	7
Asymmetry	0	0	0	0.03	0.28	0.44	0.78

In comparison to the UG2UG channel, it is seen that these links are more asymmetrical. The transitional region for the AG2UG channel ranges from 4.18 meters to 7 meters (2.82 meters) and for the UG2AG channel from 7 meters to 11 meters (4 meters).

6.5.4 RSS, LQI and PRR in Wet Scenario

As expected, the increased VWC results in increased path loss for links in both channels. The communication ranges for links in the UG2AG channel reduced by 32%, whilst the communication ranges for links in the AG2UG channel reduced by 27%. The RSS variance is consistent with the dry scenario, therefore the increase in VWC has no apparent effect on the RSS temporal characteristics. The observed behaviour for LQI differs. In the dry case, it was observed that the LQI mean could be low for very close inter-node instances (i.e. 1 meter), but for corresponding inter-node distances in the wet scenario the mean is much higher than in the dry scenario. This can be caused by the fact that a higher VWC affects the properties of the air-soil/ soil-air interfaces, since the soil's refractive index is dependent on the VWC. The difference in PRR in the wet scenario causes a slight difference in transitional region width for links in both channels, which indicates that higher VWC slightly decreases the asymmetry.

6.6 SUMMARY OF RESULTS

Links in the UG2UG channel exhibit high quality traces (i.e. extremely RSS high temporal stability and high link symmetry), but are subject to very limited communication ranges. An increase in VWC does not affect LQI and RSS temporal characteristics in UG2UG links. Overall, the RSS is very stable and the LQI is highly variant, and not correlated with RSS nor PRR. The temporal characteristics of links in AG2UG and UG2AG channels are comparable to links in OTA channels. It is observed that the LQI behaviour for these links differs from UG2UG links, and also differs in dry and wet scenarios. In UG2UG links, the LQI has an inverse relationship with inter-node instance. This can be attributed to the fact that the effect of reflections due to the soil-air interface decreases as the inter-node distance increases. Since the soil's relative permittivity changes in wet conditions, the effect of the air-soil and soil-air interfaces also changes as the transmission and reflection losses are dependent on the soil's permittivity. Therefore, the difference observed in LQI behaviour for AG2UG and UG2AG links can be attributed to this change in permittivity. However, comprehensive models for the time and angular dispersion of signals at these interfaces are required before the actual effect can be adequately evaluated.

CHAPTER 7 CONCLUSION AND FUTURE RESEARCH

7.1 CONCLUSION

The goal of this research was to analyse the link quality characteristics of WUSNs. To this end, a simple test-bed was used to conduct an experimental investigation, where links belonging to the three communication channels of WUSNs were evaluated in both dry and wet conditions. This study was motivated by the fact that an understanding of link quality is a fundamental building block for protocol development. Since communication in WUSNs occurs over three different types of channels, it is necessary to determine the link quality characteristics of each channel for efficient protocol development.

The results of this research show that:

- Links in the UG2UG channel exhibit very high temporal stability in terms of RSS, are symmetric, and have high PRRs even for RSS values near the receiver sensitivity, but are severely limited to small communication ranges. In wet conditions, the path loss is higher, therefore affecting the RSS spatial characteristics and PRR, with no significant effect on LQI. Temporal characteristics for both LQI and RSS remain unchanged in wet conditions.
- Links in AG2UG and UG2AG channels exhibit temporal stability comparable to OTA channels, and also comparable PRRs for corresponding RSS values, but are generally asymmetric.
- The LQI for all three channels is highly variant and inconsistent and is therefore not a reliable metric for WUSNs. In the UG2UG case, it was observed that the LQI mean decreases with increasing inter-node distance, but this was not observed in the UG2AG and AG2UG channels. The LQI is very sensitive to the effects of the air-soil and soil-air interfaces. Further modelling and experimentation is required to evaluate the actual effects of the air-soil and soil-air interfaces on LQI.

The results from this research have some evident consequences on protocol development for WUSNs. The high stability of the UG2UG channel can be exploited for fast link quality estimation. For instance, RSS based link quality estimation with a single packet is sufficient to determine which forwarding link to select. Additionally, this high temporal stability enables very stable topologies, therefore reducing the number of exchanged messages for topology management. For the UG2AG/AG2UG channels, the inherent asymmetry can be exploited by metrics which favour uni-directional links such as ETF, as PRR based bi-directional estimators such as ETX discriminate against highly asymmetric links. Finally, environmental awareness has to be integrated into communication protocols. For instance, in dry scenarios, transmit power can be minimized while maintaining the same level of connectivity, but the WUSN has to be aware of the moisture content in soil in order to be able to trigger such an action. Awareness of irrigation times and predicted weather can also aid in creating more efficient WUSNs. It is evident that novel communication protocols specifically suited for WUSNs have to be developed.

7.2 FUTURE RESEARCH

For link quality characterization specifically, a complete characterization of the transmission losses at the soil-air and air-soil interfaces for the UG2AG and AG2UG channels is required. For instance, when the soil moisture is increased due to irrigation or rain, the soil's permittivity changes and the magnitude of these losses are affected by this change. Furthermore, comprehensive models for the time and angular dispersion of signals crossing these interfaces are required, so that their actual effect on link quality characteristics (LQI in particular) can be evaluated. Efficient integration of environmental awareness, from a hardware and software perspective, has to be investigated. From a general WUSN perspective, other research efforts are worth investigating.

Retrieving buried nodes to replace batteries is not feasible. Hence, energy harvesting techniques have to be investigated. Potential sources of energy include vibrations from tractors or wireless power transfer techniques. These methods have to be optimized for WUSNs specifically, and novel methods have to be investigated. In particular, the use of a

secondary ultra-low power radio is worth investigating, so that low duty cycle protocols can be implemented.

Given its high temporal stability, RSS can be used to sense changes in moisture. Since an increase in moisture effectively results in a decrease in RSS, the correlation between these two parameters can be exploited for moisture sensing. Such an approach can reduce the deployment cost as sensing is then done by tracking signal variations, and no dedicated moisture sensors are necessary. This in turn simplifies the inclusion of environmental awareness into communication protocols as no additional hardware is used.

REFERENCES

[1] I. Akyildiz, W. Su, Y. Sankarasubramaniam and E. Cayirci, "Wireless sensor networks: a survey," *Elsevier Computer Networks*, vol. 38, no. 4, pp. 393 – 422, Mar. 2002.

[2] "10 Emerging Technologies That Will Change the World: Wireless Sensor Networks". Available: http://www2.technologyreview.com/featured-story/401775/10-emerging-technologies-that-will-change-the/2/. Last accessed in Dec. 2013.

[3] B. Warneke, M. Last, B. Leibowitz and K. Pister, "Smart Dust: communicating with a cubic-millimeter computer," *Computer*, pp. 44 – 51, Jan. 2001.

[4] G.P. Hancke, B. de Carvalho e Silva, G.P. Hancke Jr., "The Role of Advanced Sensing in Smart Cities," *Sensors*, 2013.

[5] C. Alcaraz, P. Najera, J. Lopez and R. Roman, "Wireless sensor networks and the Internet of Things: Do we need a complete integration?," in *Proc. of the 1st Int. Workshop on the Security of the Internet of Things (SecIoT'10)*, 2010.

[6] "WSN Chipset Shipments Will Surpass 1 Billion by 2017", Available: http://onworld.com/news/news1Billionchipsets.html. Last accessed in Jan. 2014.

[7] J. Heidemann, M. Stojanovic and M. Zorzi, "Underwater sensor networks: application, advances and challenges," *Philosophical Transactions of the Royal Society A*, pp. 158 – 175, Aug. 2012.

[8] I. Akyildiz and E. Stunbeck, "Wireless Underground Sensor Networks: Research Challenges," *Elsevier Ad Hoc Networks*, vol. 4, no. 6, pp. 669-686, Nov. 2006.

[9] S. Yoon, L. Cheng, E. Ghazanfari, S. Pamakcu and M. Suleiman, "A Radio Propagation Model for Wireless underground Sensor Networks," in *Proc. of IEEE Global Telecommunications Conf. (GLOBECOM)*, pp. 1-5, 5-9 Dec. 2011.

[10] H. Xiaoya, G. Chao, W. Bingwen and X. Wei, "Channel Modeling for Wireless Underground Sensor Networks," in *Proc. of IEEE 35th Annual Computer Soft. And Applications Conf.*, pp. 249-254, 18-22 Jul. 2011.

[11] J. Tiusanen, "Attenuation of a Soil Scout Radio Signal," *Elsevier Biosystems Engineering*, vol. 90, no. 2, pp. 127-133, 2005.

[12] Z. Sun, "Reliable and Efficient Communications in Wireless Underground Sensor Networks," Doctoral Dissertation, *Georgia Institute of Technology*, Atlanta, Georgia, 2012.

[13] A. Silva and M. Vuran, "Development of a Testbed for Wireless Underground Sensor Networks," *EURASIP Journal of Wireless Communications and Networking*, vol. 2010, pp. 1-14, 2010.

[14] A. Silva and M. Vuran, "Communication with Aboveground devices in Wireless Underground Sensor Networks: An Empirical Study," in *Proc. of IEEE Int. Conf. on Communications (ICC)*, pp. 1-6, 23-27 May 2010.

[15] H. Karl and A. Willig, "Protocols and Architecture for Wireless Sensor Networks," *Wiley*, 2006.

[16] X. Dong and M. Vuran, "Empirical analysis of the hidden terminal problem in Wireless Underground Sensor Networks," in *Proc. of Int. Conf. on Wireless Communications in Unusual and Confined Areas (ICWCUCA)*, pp. 1-5, 28-30 Aug. 2012.

[17] J. Tooker and M. Vuran, "Mobile data harvesting in wireless underground sensor networks," in *Proc. of 9th Annual IEEE Communications Society Conf. on Mesh and Ad Hoc Networks (SECON)*, pp. 560 – 568, 18-21 Jun. 2012.

[18] A. Adel and F. Norsheila, "Probabilistic routing protocol for a hybrid wireless underground sensor network," *Wireless Communications and Mobile Computing*, vol. 12, no. 2, pp. 142-156, Feb. 2013.

[19] D. Lymberoupoulos, Q. Lindsey and A. Savvides, "An empirical characterization of radio signal strength variability in 3-d IEEE 802.15.4 networks using monopole antennas," in *Proc. of the 3rd European Conf. on Wireless Sensor Networks (EWSN)*, pp. 326 – 341, 2006.

[20] C. Boano, T. Voigt, A. Dunkels, F. Osterlind, N. Tsiftes, L. Motolla and P. Suarez, "Exploiting the LQI variance for rapid channel quality assessment," in *Proc. of Int. Conf. on Information Processing in Sensor Networks (IPSN)*, pp. 369-370, 13-16 April 2009.

[21] M. Borges, F. Velez and A. Lebres, "Survey on the Characterization and Classification of Wireless Sensor Networks Applications," *IEEE Communication Surveys and Tutorials*, vol. 16, no. 4, pp. 1860 - 1890, 2014.

[22] J. Horneber and A. Hergenroder, "A Survey on Testbeds and Experimentation Environments for Wireless Sensor Networks," *IEEE Communication Surveys and Tutorials*, vol. 16, no. 4, pp. 1820 - 1838, 2014.

[23] S. Sudevalayam and P. Kulkarni, "Energy Harvesting Sensor Nodes: Survey and Implications," *IEEE Communications Surveys & Tutorials*, vol. 13, no. 3, pp. 443-461, 2011.

[24] F. Ferrari, "Sensor Networks: Where Theory Meets Practice," *Springer*, 2009.

[25] W. Dargie and C. Poellabauer, "Fundamentals of Wireless Sensor Networks: Theory and Practice," *Wiley*, 2010.

[26] IEEE, Std. 802.15.4 – 2003, "Wireless Medium Access Control (MAC) and Physical Layer (PHY) Specifications for Low Rate Personal Area Networks (WPAN)," 2003.

[27] W. Ye, J. Heidemann and D. Estrin, "An energy-efficient MAC protocol for wireless sensor networks," in *Proc. of the 21st Annual Joint. Conf. of the IEEE Comp. and Com. Soc. (INFOCOM)*, pp. 1567 – 1576, Jan. 2002.

[28] P. Lin, C. Qiao and X. Wang, "Medium Access Control with a Dynamic Duty for Sensor Networks," in *Proc. of IEEE Wireless Communications and Networking Conf. (WCNC)*, pp. 1534 – 1539, 21-25 Mar. 2004.

[29] J. Polastre, J. Hill and D. Culler, "Versatile Low Power Media Access for Wireless Sensor Networks," *in Proc of the 2nd Int. Conf. on Embedded networked sensor systems (SenSys)*, pp. 95 – 107, 3-5 Nov. 2004.

[30] V. Rajendran, K. Obraczka and J. Garcia-Luna-Neves, "Energy-efficient collision-free medium access control for wireless sensor networks", *in Proc of the 1st Int. Conf. on Embedded networked sensor systems (SenSys)*, pp. 181 – 192, 5-7 Nov 2003.

[31] N. Pantazis, S. Nikolidakis and D. Vergados, "Energy-Efficient Routing Protocols in Wireless Sensor Networks: A Survey," *IEEE Communications Surveys & Tutorials*, vol. 15, no. 2, pp. 551 – 591, 2013.

[32] K. Akkaya and M. Younis, "A survey on routing protocols for wireless sensor networks," *Ad Hoc Networks*, vol. 3, no. 3, pp. 325 – 349, May 2005.

[33] K. Yu, T. Zheng, Z. Pang, M. Gidlund, J. Åkerberg and M. Björkman, "Reliable flooding-based downlink transmissions for Industrial Wireless Sensor and Actuator Networks," in *Proc. of IEEE Int. Conf. on Industrial Technology (ICIT)*, pp. 1377-1384, 25-28 Feb. 2013.

[34] D. De Couto, D. Aguayo, J. Bicket and R. Morris, "A high-throughput path metric for multi-hop wireless routing," in *Proc. of the 9th Int. Conf. on Mobile Computing and Networking (MobiCom)*, pp. 134 – 139, 14-19 Sep. 2003.

[35] W. Heinzelman, A. Chandrakasan and H. Balakrishman, "Energy-efficient communication protocol for wireless microsensor networks," in *Proc. of the 33th Annual Hawaii Int. Conf. on System Sciences*, pp. 1-10, 4-7 Jan. 2000.

[36] I. Akyildiz and M. Vuran, "Wireless Sensor Networks," *John Wiley and Sons*, 2010.

[37] W. Chonggang, K. Sohraby, B. Li, M. Daneshmand and Y. Hu, "A survey of transport protocols for wireless sensor networks," *IEEE Network*, vol. 20, no. 3, pp. 34 – 40, May 2006.

[38] C. Wan, A. Campbell and L. Krishnamurthy, "Pump-slowly, fetch-quickly (PSFQ): a reliable transport protocol for sensor networks," *IEEE Journal on Selected Areas in Communications*, vol. 23, no. 4, pp. 862-872, April 2005.

[39] T. Lennvall, S. Svensson and F. Hekland, "A Comparison of WirelessHART and ZigBee for Industrial Applications," in *Proc. of IEEE Int. Workshop on Factory Communication Systems (WFCS)*, pp. 85-88, 21-23 May 2008.

[40] S. Petersen and S. Carlsen, "WirelessHART Versus ISA100.11a: The Format War Hits the Factory Floor," *IEEE Industrial Electronics Magazine*, vol. 5, no. 4, pp. 23 – 34, Dec. 2011.

[41] D. Schneider, "Wireless networking dashes in a new direction," *IEEE Spectrum*, vol. 47, no. 2, pp. 9 – 10, Feb. 2010.

[42] M. Weyn, G. Ergeerts, L. Wante, C. Vercauteren and P. Hellinckx,"Survey of the DASH7 Alliance Protocol for 433 MHz Wireless Sensor Communication," *Hindawi International Journal of Distributed Sensor Networks*, vol. 2013, pp. 1-9, 2013.

[43] J.P. Norair, "Introduction to DASH7 Technologies: 1st Edition," Mar. 2009.

[44] "OSS-7: Open Source Stack for Dash7 Alliance Protocol", Available: http://github.com/CoSys-Lab/dash7-ap-open-source-stack. Last accessed in April 2014.

[45] "GainSpan: Products", Available: http://www.gainspan.com/products/poverview. Last accessed in April 2014.

[46] "CC3000 SimpleLink Wi-Fi Module from Texas Instruments", Available: http://www.ti.com/product/cc3000. Last accessed in April 2014.

[47] J. Åkerberg, M. Gidlund and M. Björkman, "Future Research Challenges in Wireless Sensor and Actuator Networks Targeting Industrial Automation," in *Proc. of the 9th IEEE Int. Conf. on Industrial Informatics (INDIN)*, 26 – 29 Jul. 2011.

[48] A. Akhondi, S. Carlsen and S. Petersen, "The Role of Wireless Sensor Networks (WSNs) in Industrial Oil and Gas Condition Monitoring," in *Proc. of the 4th IEEE Conf. on Digital Ecosystems and Technologies (DEST)*, pp. 618 – 623, 13-16 April 2010.

[49] S. Villingiri, A. Ray and M. Kande, "Wireless Infrastructure for Oil and Gas Inventory Management," in *Proc. of the 39th Annual Conf. of the IEEE Industrial Electronics Society (IECON)*, pp. 5461 – 5466, Nov. 2013.

[50] A. Mainwaring, D. Culler, J. Polastre, R. Szewczyk and J. Anderson, "Wireless sensor networks for habitat monitoring," in *Proc. of the 1st ACM Int. Workshop on Wireless Sensor Networks and Applications (WSNA)*, pp. 88 – 97, 2002.

[51] H. Wang, J. Elson, L. Girod, D. Estrin and K. Yao, "Target Classification and Localization in Habitat Monitoring," in *Proc. of IEEE Int. Conf. on Acoustics, Speech and Signal Processing (ICASSP)*, pp. 844 – 847, April 2003.

[52] P. Corke, T. Wark, R. Jurdak, W. Hu, P. Valencia and D. Moore, "Environmental Wireless Sensor Networks," *Proceedings of the IEEE*, vol. 98, no. 7, pp. 1903 – 1917, Nov. 2010.

[53] A. Kumar, H. Kim and G.P. Hancke, "Environmental Monitoring Systems: A Review," *IEEE Sensors*, vol. 13, no. 4, pp. 1329 – 1339, April 2013.

[54] M. Durisic, Z. Tafa, G. Dimic and G. Milutinovic, "A survey of military applications of wireless sensor networks," in *Proc. of 2012 Mediterranean Conf. on Embedded Computing (MECO)*, pp. 169 – 199, 19 -21 Jun. 2012.

[55] S. Movassaghi, M. Abolhasan, J. Lipman, D. Smith and A. Jamalipour, "Wireless Body Area Networks: A Survey," *IEEE Communications Surveys & Tutorials*, vol. 16, no. 3, pp. 1658 – 1686, 2014.

[56] R. Bader, M. Pinto, F. Spenrath, P. Wollmann and F. Kargl, "BigNurse: A Wireless Ad Hoc Network for Patient Monitoring," in *Proc. of Pervasive Health Conf. and Workshops*, pp. 1-4, 29 Nov. – 1 Dec. 2006.

[57] Y. Kim, R. Evans and W. Iversen, "Remote Sensing and Control of an Irrigation System Using a Distributed Wireless Sensor Network," *IEEE Transactions on Instrumentation and Measurement*, vol. 57 no. 7, Jul. 2008.

[58] "Wireless Underground Sensor Networks". Available: http://www.idc.lnt.de/en/forschung/wireless-underground-sensor-networks/. Last accessed in Jun. 2014.

[59] T. Rappaport, "Wireless Communications: Principles and Practice," *Prentice Hall*, 2002.

[60] "Electromagnetic Waves and Antennas". Available: http://eceweb1.rutgers.edu/~orfanidi/ewa/. Last accessed in Jul. 2014.

[61] D. Robinson, S. Jones, J. Wraith, D. Or and S. Friedman, "A Review of Advances in Dielectric and Electrical Conductivity Measurement in Soils Using Time Domain Reflectometry," *Vadose Zone Journal*, vol. 2, no. 4, pp. 444 – 475, Nov. 2003.

[62] S. Yoon, L. Cheng, E. Ghazanfari, Z. Wang, X. Zhang, S. Pamakcu and M. Suleiman, "Subsurface monitoring using low frequency wireless signal networks,"

in *Proc. of Pervasive Computing and Communications Workshop (PerCom)*, pp. 443 - 446, 19 - 23 Mar. 2012.

[63] N. Peplinski, F. Ulaby and M. Dobson, "Dielectric properties of soils in the 0.3-1.3 GHz range," *IEEE Tranactions on Geoscience and Remote Sensing*, vol. 33, no. 3, pp. 803-807, May 2005.

[64] J. Tiusanen, "Soil Scouts: Description and performance of single hop wireless underground sensor networks," *Elsevier Ad Hoc Networks*, vol. 11, no. 5, pp. 1610 - 1618, Mar. 2013.

[65] M. Dalel, "Non-Invasive Method for Detecting Changes in Soil Moisture using Wireless Sensor Networks," Master Thesis, *Queensland University of Technology*, Brisbane, Australia, 2012.

[66] L. Li and I. Akyildiz, "Characteristics of Underground Channel for Wireless Underground Sensor Networks," in *Proc. of the 6th Annual Mediterranean Ad Hoc Networking Workshop*, pp. 92-99, 2007.

[67] Z. Sun and I. Akyildiz, "Magnetic Induction Communications for Wireless Underground Sensor Networks," *IEEE Transactions on Antennas and Propagation*, vol. 58, no. 7, pp. 2426 – 2435, Jul. 2010.

[68] Z. Sun, I. Akyildiz, S. Kisseleff and W. Gerstacker, "Increasing the capacity of Magnetic Induction Communications in RF-Challenged Environments," *IEEE Transactions on Communications*, vol. 61, no. 9, pp. 3943 – 3952, 2013.

[69] S. Kisseleff, I. Akyildiz and W. Gerstacker, "Interference Polarization in magnetic induction based Wireless Underground Sensor Networks," in *Proc. of PIMRC Workshops*, pp. 71 – 75, 2013.

[70] A. Sample, B. Waters, S. Wisdom and J. Smith, "Enabling Seamless Wireless Power Delivery in Dynamic Environments," *Proceedings of the IEEE*, vol. 101, no. 6, pp. 1343 – 1358, 19-23 Jun. 2013.

[71] A. Vlavianos, L. Law, L. Broustis, S. Krishnamurthy and M. Faloutsos, "Assessing link quality in Wireless Networks: Which is the right metric?," in *Proc. of the 19th IEEE Int. Symposium on Personal, Indoor and Mobile Radio Communications*, pp. 1-6, 15-18 Sep. 2008.

[72] M. Zuniga and B. Krishnamachari, "Analysing the transitional region in low power wireless links," in *Proc. of the 1st Annual IEEE Communications Society Conf. on Sensor and Ad Hoc Communications (SECON)*, pp. 517 – 526, 4 – 7 Oct. 2004.

[73] S. Haykin and M. Moher, "Communication Systems," 4th Edition, *John Wiley and Sons*, 2010.

[74] CC2420 2.4 GHz IEEE 802.15.4 Transceiver Datasheet, Texas Instruments.

[75] CC1101 sub 1-GHz Transceiver Datasheet, Texas Instruments.

[76] C. Boano, M. Zuniga, T. Voigt, A. Willig and K. Romer, "The Triangle Metric: Fast Link Quality Estimation for Mobile Wireless Networks," in *Proc. of the 19th Int. Conf. on Comp. Communications and Networks (ICCCN)*, pp. 1-7, 2-5 Aug. 2010.

[77] K. Srinivasan and P. Levis, "RSSI is Under Appreciated," in *Proc. of the 3rd Workshop on Embedded Networked Sensors*, pp. 499 – 503, May 2006.

[78] M. Spuhler, "Ultra-fast and Accurate Wireless Link Quality Estimation and the Benefits it Provides for Detection of Reactive Jamming," Master Thesis, *ETH Zurich*, Switzerland, 2012.

[79] A. Cerpa, J. Wong, M. Potkonjak and D. Estrin, "Temporal Properties of Low Power Wireless Links: Modelling and Implications on Multi-Hop Routing," in *Proc. of the 6th ACM Int. Symposium on Mobile Ad Hoc Networking and Computing (MobiHOC)*, pp. 414-425, 25-27 May 2005.

[80] M. Zuniga, I. Irzynska, J. Hauer, T. Voigt, C. Boano and K. Roemer, "Link Quality Ranking: Getting the best out of unreliable links," in *Proc. of Int. Conf. on Distributed Computing in Sensor Systems and Workshops*, pp. 1-8, 27-29 June 2011.

[81] R. Fonseca, O. Gnawali, K. Jamieson and P. Levis, "Four-Bit Wireless Link Estimation," in *Proc. of the 6th Workshop on Hot Topics in Networks (HotNets)*, pp. 1-5, 14-15 Nov. 2007.

[82] N. Baccour, A. Koubaa, H. Youssef, M. Jamaa, D. do Rosario, M. Alves and L. Becker, "F-LQE: a fuzzy link quality estimator for wireless sensor networks," in *Proc. of the 7th European conf. on Wireless Sensor Networks (EWSN)*, pp. 240 – 255, 17 – 19 Feb. 2010.

[83] L. Sang, A. Arora and H. Zhang, "On link asymmetry and one-way estimation in wireless sensor networks," *ACM Transactions on Sensor Networks*, vol. 6, no. 2, pp. 1-25, Feb. 2010.

[84] A. Subramanian, M. Buddhikot and S. Miller, "Interference aware routing in multi-radio wireless mesh networks," in *Proc. of the 2nd IEEE Workshop on Mesh Networks (WiMesh)*, pp. 55 - 63, 25 – 28 Sep. 2006.

[85] Y. Yang, J. Wang and R. Kravets, "Designing routing metrics for mesh networks," *in 1st IEEE Workshop on Wireless Mesh Networks (WIMesh)*, 2005.

[86] K. Wehrle, M. Gunes and J. Gross, "Modelling and Tools for Network Simulation," *Springer*, 2010.

[87] T. Issariyakul and E. Hossain, "Introduction to Network Simulator 2," *Springer*, 2009.

[88] "ns-3", Available: http://www.nsnam.org. Last accessed in Dec. 2013.

[89] "OMNeT++ Network Simulation Framework", Available: http://www.omnetpp.org. Last accessed in Dec. 2013.

[90] "Castalia Wireless Sensor Network Simulator", Available: http://castalia.forge.nicta.com.au. Last accessed in Dec. 2013.

[91] P. Levis, N. Lee, M. Welsh and D. Culler, "TOSSIM: accurate and scalable simulation of entire TinyOS applications," in *Proc. of ACM SenSys*, pp. 126-137, 2003.

[92] J. Polley, D. Blazakis, J. McGee, D. Rusk, J. Baras and M. Karir, "ATEMU: A fine-grained sensor network simulator," in *Proc. of the 1st IEEE Communications Society Conference on Sensor and Ad Hoc Networks (SECON)*, pp. 145-152, 4-7 Oct. 2004.

[93] B. Titzer, D. Lee and J. Palsberg, "Avrora: scalable sensor network simulation with precise timing," in *Proc. of 4th Int. Symposium on Information Processing in Sensor Networks*, pp. 477 – 482, 15 April 2005.

[94] "WizziLab: Connecting Things, WizziMote", Available: http://www.wizzilab.com/shop/wizzimote/. Last accessed in May 2014.

[95] E. Stunbeck, D. Pompili and T. Melodia, "Wireless Underground Sensor Networks using Commodity Terrestrial Motes," in *Proc. of the 2nd IEEE Workshop on Wireless Mesh Networks (WiMesh)*, pp. 112-114, 25-28 Sep. 2006.

[96] J. Zhao and R. Govindan, "Understanding packet delivery performance in dense wireless sensor networks," in *Proc. of the 1st Int. Conf. on Embedded Networked Sensor Systems (SenSys)*, pp. 1-13, 5 – 7 Nov. 2003.

APPENDIX A EQUATIONS FOR DETERMINATION OF SOIL PARAMETERS

Empirically determined constants (from [63])	$\beta_I = 1.2748 + 0.519S + 0.152C$ $\beta_{II} = 1.3379 - 0.603S + 0.166C$
Assumptions	$\varepsilon_{f_w}^{I}$ and $\varepsilon_{f_w}^{II}$ were computed from equations in [63] and $\alpha^I = 0.65$ [63]
Real part of complex Dielectric Constant of soil (from [63])	$\varepsilon_I = 1.15\left[1 + \frac{p_b}{p_s}\left(\varepsilon_s^{\alpha^I}\right) + m_v^{\beta_{II}}\varepsilon_{f_w}^{I\alpha^I} - m_v\right]^{\frac{1}{\alpha^I}} - 0.68$
Complex part of complex Dielectric Constant of soil (from [63])	$\varepsilon_{II} = \left[m_v^{\beta_{II}}\varepsilon_{f_w}^{II\alpha^I}\right]^{\frac{1}{\alpha^I}}$

S – sand percentage

C – clay percentage

p_b – specific density of solid soil particles (g/cm^3)

p_s – bulk density (g/cm^3)

m_v – volumetric water content (%)